Optically stimulated luminescence signals from quartz

Wintle, A. G.; Adamiec, G.

Published in:
Radiation Measurements

DOI:
10.1016/j.radmeas.2017.02.003

Publication date:
2017

Citation for published version (APA):
Wintle, A. G., & Adamiec, G. (2017). Optically stimulated luminescence signals from quartz: A review. *Radiation Measurements*, *98*, 10-33. https://doi.org/10.1016/j.radmeas.2017.02.003

Accepted Manuscript

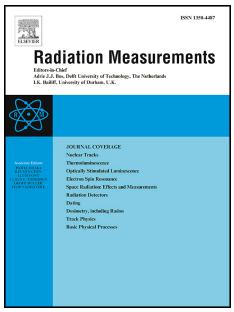

Optically stimulated luminescence signals from quartz: A review

A.G. Wintle, G. Adamiec

PII: S1350-4487(17)30093-8

DOI: 10.1016/j.radmeas.2017.02.003

Reference: RM 5706

To appear in: *Radiation Measurements*

Received Date: 5 August 2016

Revised Date: 31 January 2017

Accepted Date: 2 February 2017

Please cite this article as: Wintle, A.G., Adamiec, G., Optically stimulated luminescence signals from quartz: A review, *Radiation Measurements* (2017), doi: 10.1016/j.radmeas.2017.02.003.

Optically stimulated luminescence signals from quartz: a review

A.G. Wintle[a,b], G. Adamiec[c]*

[a] *Department of Geography and Earth Sciences, Aberystwyth University, Aberystwyth, SY23 3DB, UK*

[b] *McDonald Institute for Archaeological Research, University of Cambridge, CB2 3ER, UK*

[c] *Institute of Physics CSE, Silesian University of Technology, ul. Konarskiego 22B, 44-100, Gliwice, Poland*

Abstract

Optically stimulated luminescence (OSL) was first observed from natural quartz 30 years ago. Since it increases with exposure to radiation, OSL has been developed as a dating tool for sediments. Most commonly, the OSL signal is observed using optical filters that pass wavelengths centred on 340 nm during optical stimulation at 470 nm. Experimental evidence behind the choice of measurement conditions for dating is presented, for example, information on the emission spectra. Different methods of optical stimulation are reviewed, including non-linear application of stimulation power; these are related to isolation of the fast OSL component that is most appropriate for dating sediments. Practical methods for fast OSL component separation are mentioned. Information on the stimulation process has been obtained by varying the wavelength during measurement and by varying the stimulation temperature. On the other hand, information on the recombination process is provided by observing the OSL emitted when the stimulation source is pulsed; this has practical applications when feldspar contamination is expected. Although laboratory experiments imply more than adequate thermal stability of the fast OSL signal for dating back to a million years, ages determined in the laboratory using the single aliquot regenerative dose procedure do not agree with independent ages. To address this problem, luminescence signals derived from the same electron trap, as well as those resulting from stimulation in the infrared (875 nm) and in the violet (405 nm), have been investigated as potential dating tools.

Keywords:

Quartz, OSL, optically stimulated luminescence, stimulation spectra, emission spectra, thermal treatment

*Corresponding author: email grzesadam@gmail.com; phone +48 322372254

Contents

1. Overview

Over the past 30 years, a particular optically stimulated luminescence signal (termed the fast component) has been measured from sedimentary quartz grains and used to obtain depositional ages for the sediments. Alongside such applications, laboratory experiments have been carried out in order to establish a basis for the measurement protocols used for age determination. The first part of this review paper (sections 2-10) covers experimental work carried out primarily since 2003 when a book was published (Bøtter-Jensen et al., 2003) on Optically Stimulated Luminescence Dosimetry which had extensive sections on quartz. Also, in the last 15 years, models of OSL production in quartz have been developed, based on the numerical model of Bailey (2001), that enable prediction of experimental results and also prediction of the stability of the fast OSL signal over long periods of time, as is needed for dating.

Experimental work on methods of measurement of the OSL signals is presented in section 4 and a summary is presented in terms of what is most useful for dating procedures. In section 5, spectral measurements are reported, not just for OSL but also for associated methods of luminescence production. Although the spectra are well characterised, there is still a lack of information about the nature of the defects in natural quartz and this is mentioned in the summary of section 5. Sections 6 and 7 provide an overview of processes related to OSL production, and the conditions under which the signal may be measured in the single aliquot regenerative dose (SAR) protocol widely used to obtain ages for sediments.

However, applications to independently dated sedimentary deposits from the last 200,000 years (200 ka) have yielded underestimated OSL ages for sediments over 50 ka. This is discussed in section 8, where dose response curves for the fast component of the OSL signal are discussed. This has led to investigation of new methods of stimulating OSL which are discussed in section 9. In sections 10 and 11, the latest developments concerning other signals derived from trapped electrons are reviewed individually.

The intention of this paper is to provide an overview for doctoral students embarking on a research project on OSL of quartz, particularly when their aim is to use OSL signals to provide a chronology. The aim is to summarize what is known, and what is not known, about the OSL signals found in sedimentary quartz, with some

additional information from synthetic materials. Where experimental results have been discussed within a modelling framework this has been included in this review.

2. Introduction

When quartz grains are exposed to light following absorption of a radiation dose, an optically stimulated luminescence (OSL) signal is observed. The larger the dose, the greater is the OSL signal and this property enables quartz to be used as a dosimeter (Bøtter-Jensen et al., 2003; Preusser et al., 2009). The effective radiation dose received by quartz grains in the environment can be obtained by comparing the natural OSL signal with the OSL measured after the delivery of a dose from a calibrated, usually beta emitting, laboratory source. The signal decays rapidly when exposed to direct sunlight and increases again through absorption of environmental radiation once the quartz grains have been incorporated in a sedimentary deposit. A measurement procedure has been developed in which the effective dose received by the grains in nature, termed the equivalent dose, can be obtained for a single aliquot of quartz grains (Murray and Wintle, 2000) consisting a few hundred to a few thousand grains (Heer et al., 2012) or even for a single grain of a diameter of 100-200 μm (Jacobs and Roberts, 2007; Duller, 2008). The equivalent dose is divided by the separately measured environmental dose rate to obtain an age; in the case of sediment, this is the time since the quartz grains were last exposed to sunlight. The acquired OSL can also be erased by heating the quartz grains, e.g. during firing of ceramics, however in this review we will not consider heating as a zeroing mechanism.

The OSL signal used for dating is usually obtained under conditions of constant power density of the stimulating light source, usually at blue or green wavelengths, most frequently of the order of a few tens of mW/cm^2, resulting in a continuous wave OSL (CW-OSL) signal. Since the discovery of OSL by Huntley et al. (1985), significant effort has been put into explaining the processes taking place in quartz in order to provide a theoretical framework for establishing the accuracy of protocols used for determining the absorbed dose. This research is difficult due to several reasons, the main ones being the low intensity of the signal and the wide variability of luminescence properties between different samples or even grains of the same sample (Adamiec, 2000a; Jacobs et al., 2003; Arnold and Roberts, 2011).

A comprehensive summary of OSL properties of quartz was provided by Bøtter-Jensen et al. (2003 pp. 119-188). Since then, Wintle and Murray (2006) published a review of the use of quartz as a dosimeter using the single-aliquot regenerative-dose (SAR) dating protocol; this also summarised experimental evidence for various phenomena related to this application. In particular, OSL dating of recent geological sediments has been widely adopted, as reviewed in a number of papers in issue 4 of volume 7 of the journal Boreas (e.g. Roberts, 2008) and it is also used for sediments containing archaeological remains, as reviewed by Roberts et al. (2015). Preusser et al. (2009) reviewed the luminescence properties of quartz, relating them to current knowledge of the structure of quartz and its geological origin, with special consideration of identified lattice defects. Limitations in the ability to use OSL signals with ages over 100 ka have led to the investigation of other OSL signals in quartz, such as thermally transferred OSL (TT-OSL, i.e. OSL induced by heating following a bleaching of the previously acquired signal). This topic has recently been the subject of a review article by Duller and Wintle (2012). An overview of models and simulations of TL and OSL production has been provided by Chen and Pagonis (2011). Schmidt et al. (2015) reviewed radioluminescence (RL) in quartz; RL can provide valuable information about the luminescence centres that participate in OSL and TL production. Time-Resolved (TR-OSL) studies, primarily of synthetic quartz, have been the subject of a recent review by Chithambo et al. (2016); TR-OSL provides information on the lifetimes of the processes that control OSL production.

3. Physical mechanisms of luminescence production in crystals

Due to quantum mechanical properties, electrons in crystals can have energies that are within energy bands that originate from the orbitals of atoms forming the crystal lattice. The bands that play a role in movement of electrons are the valence and conduction bands. Electrons that have energies within the conduction band can move practically freely in the volume of the crystal. In insulators, like quartz, the conduction band is very well separated from the valence band and normally no electrons are able to move through the crystal; thus, no electricity is conducted. However, when a crystal absorbs energy greater than the bandgap width (the energy difference between the conduction and the valence band edge), free electrons are created in the crystal volume. These electrons are mobile within the conduction band; in the absence of any metastable states, they typically recombine with the holes in the

valence band by a stepwise loss of energy. In crystalline quartz, the distance in the energy domain between the valence band and the conduction band edge, i.e. the energy band-gap, has been determined to be about 8.7 eV (Quinn et al., 2003). The conduction and valence bands are referred to as delocalised because they extend through the whole volume of the crystal.

Real crystals are characterised by a number of defects, i.e. imperfections of the crystal lattice. They stem either from the intrusion of impurity atoms, or from structural faults. Such defects give rise to localised energy states because their orbitals do not align with the orbitals of the atoms creating the lattice, and hence, at the location of the defect, electrons can take energy values forbidden in the remainder of the crystal. At those locations (metastable states, also called traps) the movement of electrons is inhibited. Depending on the type of the trap, electrons can remain there at ambient temperature even for millions of years, a property exploited in luminescence dating. Additional energy through heating or illumination needs to be supplied to evict the electrons into the conduction band where they can move freely.

When an electron is excited from the valence band to the conduction band, in the valence band there is a lack of an electron, called a hole – this is a quasiparticle with a positive charge and positive mass. Similarly, in the forbidden gap, energy levels may exist close to the top of the valence band where electrons can be missing, forming electron-hole recombination centres. When an electron moving in the conduction band finds itself in the proximity of such a recombination centre, it loses energy recombining with the centre and may emit light – in such a case the centre is called a luminescence centre. Such trapping sites or recombination sites are localised because they occupy a particular place in the crystal. In feldspars, recombination can occur directly between electron trapping sites and recombination centres when they are close to one another due to quantum mechanical tunnelling. However, to date, there is no evidence of the existence of such transitions in quartz.

Figure 1 (from Bailey, 2001) Energy level diagram showing different traps and recombination centres and allowable transitions.

An energy band model is used to illustrate how TL and OSL are produced, and a version used for quartz was produced by Bailey (2001). This model, together with the accompanying mathematical treatment and selected parameters (such as trap depth

energies) allow prediction of the behaviour of TL and OSL signals. Bailey's model (Fig. 1) shows electron trapping centres denoted by the suffix i (i = 1-5) at different depths below the conduction band. Hole trapping centres, denoted by the suffix j (j = 6-9) are closer to the valence band. The vertical position of each centre indicates the energy of each trapped charge. Recently, Peng and Pagonis (2016) and Friedrich et al. (2016) have provided tools written in R to facilitate the modelling of luminescence in quartz.

As mentioned above, the excitation of electrons from valence to conduction band can occur due to the action of ionising radiation. In the energy level diagram (Fig. 1) this transition is shown by a vertical arrow on the right side. The release of electrons from the electron trapping site can be caused by the delivery of heat (i.e. through vibrations of the crystal lattice) or exposure to photons of a sufficient energy. These are shown as upward-pointing arrows from the traps to the conduction band (Fig. 1). Electrons in the conduction band can recombine with holes in recombination centres producing light in the case of luminescent centres. This process is shown by a downward-pointing arrow from the conduction band to the luminescence centre (L-centre, j = 8). There are three other recombination centres, with a transition to the killer centre (K-centre, j = 9) which is thermally stable and competes for electrons from the conduction band. The two other recombination centres (R centres, j = 6 and 7) are thermally unstable (being closer to the valence band than either the L or K centres). The recombination with each of the recombination centres may be radiative which would be seen as different wavelengths appearing in the spectrum of the emitted luminescence. When the stimulation of electrons is brought about by heating the emitted luminescence is called thermoluminescence (TL) and when by illumination with light optically stimulated luminescence (OSL).

For most sedimentary quartz, the OSL decays rapidly on a timescale of seconds (Fig. 2a); this initial part of the signal is referred to as the fast component. The initial decrease in signal can be fitted with a simple exponential function; such a decay matches the theoretical prediction for electron trap emptying with negligible re-trapping, as obtained for a one trap/one recombination centre model, i.e. first order kinetics (Bøtter-Jensen et al., 2003 pp. 28-29). The decay rate of an OSL signal is characterised by the incident photon flux of the stimulating light (Bulur et al., 2001a) and the photoionisation cross-section of the trap for the incident photon energy (Spooner, 1994; Ditlefsen and Huntley, 1994).

In reality, in quartz the recombination process has two stages. When the electrons reach the luminescence centres having left the conduction band, the centres are put in an excited state. Relaxation of the luminescence centre from its excited state to the ground state may result in the emission of a photon of a wavelength shorter than the stimulating light (known as anti-Stokes emission). These processes have been investigated by Ankjærgaard and Jain (2010) using time-resolved OSL (TR-OSL) since this can provide measurements on timescales enabling observation of these processes (see section 6). This study also provided information on long-lived phosphorescence caused by re-trapping and thermal emptying of shallow traps, a process that is frequently ignored in the analysis of luminescence signals.

4. OSL measurement and component separation

a. Continuous wave OSL (CW-OSL)

One of the possible explanations for the CW-OSL not being characterised by a single exponential function is the existence of more than one optically active traps (Bailey, 1997). Traps with a smaller photoionisation cross-section will empty more slowly and be observed at longer stimulation times. From the first OSL measurements (Huntley et al., 1985), it was clear that the decrease in OSL emission with continuous stimulation does not follow a single exponential function. Smith et al. (1986) were the first to demonstrate that the initial part of the OSL signal was related to the 325°C TL peak (as obtained using a heating rate of 5°C/s). Smith and Rhodes (1994) identified two OSL components that dominated the early part of the signal and they termed them the fast and medium components.

An additional slow component was identified by Bailey et al. (1997), and this, together with the need to describe OSL sensitivity changes, led to the development of a model for TL and OSL production mentioned in the previous section (Bailey, 2001). This model used 5 electron traps and 4 recombination centres. In Fig. 1, the electron traps giving rise to the fast and medium components are OSL_F (i=3) and OSL_M (i=4), and there is a deep trap that is optically insensitive Deep (i=5). The remaining 2 traps were related to the prominent TL peaks at 110 and 230°C (as obtained using a heating rate of 5°C/s). The trap for the 110°C TL peak had already been shown to be both light sensitive (Bailey, 1997; Wintle and Murray, 1997) and able to trap electrons through phototransfer (i.e. trapping of electrons released into the conduction band from other traps through illumination with light) during the production of the fast

OSL signal (Smith and Rhodes, 1994; Wintle and Murray, 1997). Bailey's (2001) model has been extended by Adamiec (2000a, 2005a) by an additional, thermally unstable recombination centre to explain a wider range of the observed thermally induced sensitivity changes in quartz TL. The emission peak of the thermally stable, radiative recombination centre is located at 365 nm in the near UV (Huntley et al., 1991) and this has been related to the emission spectra found for the 110, 230 and 325°C TL peaks (Franklin et al., 1995). Detailed discussion of spectra of luminescence emission is discussed in section 5.

Bailey (2000) had also observed an additional slow component after heating to 500°C. This led to the incorporation of additional slow OSL components to update the energy band model for TL and OSL production (Bailey, 2002, 2004). Further OSL studies have indicated that there are at least 3 slow components (Singarayer and Bailey, 2004), if not 4 (Singarayer and Bailey, 2003; Jain et al., 2003), each having a photoionisation cross-section that is about a factor of 10 smaller than the previous one, thus covering 4 orders of magnitude from the fast component to the slowest (Jain et al., 2003; Wintle and Murray, 2006).

Separation of a 'clean' fast OSL component is thought to be required for reliable dating, as it is rapidly zeroed by sunlight and has sufficient thermal stability for dating the last few million years (Wintle and Murray, 2006; Wintle, 2010). In their study of Japanese loess, Watanuki et al. (2005) separated their CW-OSL signals from fine grained quartz into 3 components each decaying exponentially. Using the fast component, they reported ages in agreement with independent ages back to 200 ka. Algorithms for fitting multiple components have been developed by Bluszcz and Adamiec (2006), and Kreutzer et al. (2012). Rather than applying fitting procedures to individual decay curves, Cunningham and Wallinga (2009) characterised the decay rates of the fast and medium components for each sample, using a large number of aliquots with each being given the same dose. Applying the average decay rates obtained from these measurements, an algorithm was applied to derive the equivalent dose from the fast component obtained from standard SAR measurements. This approach was particularly useful for quartz from young sediments and could be applied to both well-bleached and poorly-bleached sediments.

Instead of applying curve fitting, the equivalent dose has been determined using the signal integrated during the fast decaying part of the decay curve with an appropriate background subtracted. A standard approach is to use the late background

(as described by Banerjee et al., 2000) where the background contribution during the initial decay is estimated on the basis of the number of counts recorded at a time much larger than the fast OSL decay time constant. Another approach has been considered in which different integrals are subtracted; this was first suggested by Aitken and Xie (1992) for IRSL signals from fine grains from very young sediments and was subsequently applied by Lang and Wagner (1997). A similar approach was subsequently applied to quartz OSL signals by Ballarini et al. (2007); in this, the contribution of the background was determined using the signal recorded immediately after the period used to estimate the magnitude of the fast component. The latter approach, termed early background subtraction, may be appropriate when the contribution of the medium and slow component is significant at the beginning of the OSL decay. In an in-depth study, Cunningham and Wallinga (2010) found the application of an early background subtraction approach, using the interval immediately after that being used as the signal and one which is 2.5 times the signal interval, to be most effective.

Choi et al. (2003) and Jain et al. (2003) reported the existence of a thermally unstable ultrafast component in quartz extracted from marine terrace sediments on the south-eastern coast of Korea. The properties of this ultrafast component have been studied in depth by Jain et al. (2008). They found that the optical cross-section of the responsible source trap under blue light stimulation is about 14 times larger than that of the fast component. However, this component has been rarely reported in the literature, one exception being the study of young overbank deposits of the River Waal (Wallinga et al., 2010). For dating, they adopted the suggestion of Jain et al. (2008) that it could be easily eliminated by IR bleaching above room temperature.

b. Linearly modulated OSL (LM-OSL) and hyperbolically modulated OSL (HM-OSL)

Besides measuring CW-OSL, the OSL signal obtained using a linearly increasing stimulation power has been measured (Bulur et al., 2000, 2001a). The resulting linearly modulated OSL (LM-OSL) curve is then separated into components, assuming that the signal is made up of a finite number of first-order components (Singarayer and Bailey, 2003, 2004; Jain et al., 2003; Kitis and Pagonis, 2008).

Figure 2 a) an example of a CW-OSL decay curve with a fitted fast and medium component shown (from Wang et al. 2012) b) LM-OSL curves of seven samples and c) deconvolution of the LM-OSL curve from sample SL203 (from b) into 5 first order components (both b and c from Singarayer and Bailey, 2003).

Examples of LM-OSL curves are given in Figs. 2b and c for seven different sedimentary quartz samples measured under the same conditions (namely using 470 nm stimulation at 160°C, following a dose of 20 Gy and a laboratory heating to 260°C). It can be seen that each sample has a relatively fast OSL component, peaking after about 40 s of ramped optical stimulation. In addition, there is a much slower component, peaking after about 2000 s of on-going ramped stimulation power. However, the relative contributions vary from sample to sample, as shown by the relative heights of the peaks in these plots. In Fig. 2c, one of the curves has been fitted with 4 components which have peaks during the stimulation time, plus another even slower component.

More recently, fundamental studies using LM-OSL have been carried out on quartz grains, both from large rock crystals (Kiyak et al., 2007, 2008) and sedimentary deposits (Kitis et al., 2007, 2010a, 2011; Polymeris et al., 2009). Li and Li (2006) used LM-OSL measurements for equivalent dose determination with a single aliquot procedure for sedimentary quartz. However, although they demonstrated the viability of the procedure by showing that the equivalent doses were in agreement with those obtained using the initial part of the CW-OSL decay curve, it has not been widely adopted. This is because of the greater time required to make the LM-OSL measurements and the extra time needed for analysis compared with using CW-OSL. LM-OSL measurements have also been made on single grains of quartz from sedimentary deposits (Bulur et al., 2002).

Huntley (2006) and Jain and Lindvold (2007) have demonstrated that LM-OSL does not provide improved separation of components compared to CW-OSL, however, the components are easier to visualise in LM-OSL measurements where they appear as peaks (e.g. Bos and Wallinga, 2012). The fitting of a sum of exponential functions to a decaying function is mathematically equally difficult as fitting an LM-OSL curve with a sum of relevant components. For example, Adamiec

(2005b) discussed possible difficulties in fitting decay curves with sums of exponential functions.

Whether there is a preferred stimulation mode (CW, LM or other) for decomposing a multi-component OSL signal was addressed by Bos and Wallinga (2009a). They simulated the OSL signal resulting from a first order (i.e. no re-trapping) electron trap obtained using several different modes of stimulation, including CW-OSL and LM-OSL. They then combined two such signals with different photoionisation cross-sections and different initial trapped electron concentrations. Provided the time-integrated number of photons is the same (i.e. the total amount of energy received by the samples is the same), they confirmed that the ratio of the two components remains the same. Wallinga et al. (2008) compared the component separation obtained using CW-OSL, LM-OSL and hyperbolically-modulated OSL (HM-OSL) using measurements on quartz. They concluded that HM-OSL might be preferable when high resolution was required at the beginning of the stimulation, e.g. if an ultrafast OSL component was present.

c. OSL using frequency modulated pulsed stimulation

In an alternative approach to ramping the stimulation power, 10 μs wide pulses with a repetition rate that can be varied over frequencies between 0 and 10 kHz were used to vary the power of stimulation (Bulur et al., 2001b). The pulse intensity is kept constant, but the off time between the pulses is progressively decreased. This approach has been termed frequency modulated pulsed stimulation (FMPS) and was applied to a sample of sedimentary quartz (ibid.). The potential advantage of this approach is that there is better control of the power than in the case of LM-OSL; however, potential problems might arise if detrapping follows non-first order kinetics.

d. CW-OSL using ramped sampling period

Another experimental approach that has several potential advantages is to acquire the data whilst ramping the sampling period whilst stimulating with a fixed power source. Under this condition, the signal (ramped sample period OSL, RSP-OSL) decreases with stimulation power but when displayed as a function of collection channel has a peak similar to that of the LM-OSL. This approach was developed by Poolton et al. (2003) and applied by them to several samples of sedimentary quartz. They measured the RSP-OSL over 2455 s, linearly ramping the sample period from 0 to 7.1 s in 10

ms increments with the power of the excitation source set at 45 mW cm^{-2}. The RSP-OSL was compared with the LM-OSL signal obtained by linearly ramping the excitation power from 0 to 45 mW cm^{-2} in 4910 s with a constant sampling period of 4.9 s. Fig. 3a shows the data as a function of collection channel for a sample of quartz from Scotland, taken as an example with a dominant slow component. Fig. 3b shows the LM-OSL as a function of ramped stimulation time and Fig. 3c shows the RSP-OSL as a function of time obtained using a mathematical transformation. The displays are visually similar and result in similar detrapping parameters for the fast and slow components, but the RSP-OSL was collected in half the time. In addition, this approach can be used to separate isothermal TL signals and OSL signals made under optical stimulation when no preheat is applied immediately after irradiation (Poolton et al., 2003), but this approach has not been further pursued.

Figure 3 (from Poolton et al., 2003) comparing LM-OSL with RSP-OSL of a quartz sample, a) as the data are collected, b) LM-OSL as a function of stimulation time and c) RSP-OSL after a mathematical transformation enables the data to be plotted as a function of time.

e. Mathematically-transformed OSL signals

Besides using experimental procedures to attempt the visualization of the components, various mathematical transformations have been applied to data sets from CW-OSL measurements to provide pseudo-OSL signals. CW-OSL measurements have the advantage of having the best signal-to-noise ratio (Wallinga et al., 2008) and being the most rapid to perform. For example, mathematical transformations have been applied to create a pseudo-LM-OSL display (Bulur, 2000). Ankjærgaard et al. (2010) carried out a rigorous analysis of the numerical fitting methods applied to exponential decays, e.g. CW-OSL, and equivalent data sets obtained as a set of peaks, e.g. LM-OSL. They mainly used artificial data sets in order to provide a direct comparison and to control the noise associated with both the signal and the detector background. They also investigated the transformation of data from CW-OSL to pseudo-LM-OSL and concluded that this approach gave better results than using direct LM-OSL measurements. Using a sample of sedimentary quartz, Kitis et al. (2011) made both CW-OSL and LM-OSL measurements. They chose stimulation times and intensities for the two measurements so that the LM-OSL

curves could be directly compared with the pseudo-LM-OSL curves that they obtained from the CW-OSL data set. Their subsequent component analysis demonstrated the equivalence of the factors derived from the two data sets.

Bos and Wallinga (2012) have suggested that a pseudo-HM-OSL transformation (Bos and Wallinga, 2009a) has an advantage for observation of the fast OSL component. Bos and Wallinga (2009b) have also proposed a mathematical transformation based on the assumption that each OSL component is the result of first order kinetics. In this method, the CW-OSL decay curve is differentiated, resulting in an output similar to an LM-OSL curve.

f. Summary

From consideration of the above approaches, it must be concluded that raw data from CW-OSL measurements provides the best data set for subsequent analysis of individual components. Both conventionally measured CW-OSL and measurement of CW-OSL using a ramped sampling period to obtain the RSP-OSL are acquired in similar times; however, the latter method of measurement has the advantage that it can be used to provide a display with peaks whilst rejecting isothermal TL signals.

5. Luminescence emission

Measurements of the emission spectra of TL and OSL emissions provide important information about the transitions that occur within the luminescence centres. Due to the fact that luminescence of quartz is usually very weak, spectral measurements are challenging and optimisation of the light collection system used is needed. This is particularly true for measurements of natural quartz. A number of studies have been focused on measuring spectra of synthetic quartz, where the luminescence intensity is higher and the type of impurities can be controlled. Measurements of OSL emission spectra pose an additional challenge to TL emission spectra as separation of the emitted light from the strong stimulating light is needed. Other approaches are the measurements of RL and ionoluminescence (IL) spectra. In the following subsections, we discuss different types of spectral measurements; the results are given either as a function of energy or wavelength, the conversion formula being $E(\mathrm{eV}) \cong \frac{1239.8}{\lambda(\mathrm{nm})}$.

a. OSL emission spectra

Three broad emission bands (360-420, 420-490, 590-650 nm) have been reported in the TL emission spectra of natural quartz as reviewed by Krbetschek et al. (1997) and by Bøtter-Jensen et al. (2003 pp. 150-155). Using optical stimulation at 647 nm, Huntley et al. (1991) found the OSL emission of a natural quartz to be centred at ~365 nm, with only weak emission between 400 and 500 nm. These results showed that it is possible to observe this anti-Stokes emission by using a colour glass filter, e.g. Hoya U340 with a maximum of transmission at 340 nm (Bøtter-Jensen et al., 2000). When automated luminescence measuring systems are used and TL measurements are made in the same experimental sequence as the OSL measurements, it is usual to employ the same filter in both cases due to hardware limitations. In such cases information on both TL and OSL spectral emission is important. Automated measurements that include changing filters during the execution of a measurement sequence have been made possible by Lexsyg system (Richter et al., 2013) and Risø (Lapp et al., 2015) which should result in more studies investigating both emissions.

Since the luminescence of natural quartz is weak, most studies of OSL spectra have been carried out on slices of synthetic quartz. Martini and Galli (2007) used optical stimulation at 470 nm and a CCD detector coupled to a monochromator to observe the OSL emission spectrum in the range between 250 and 410 nm, finding it peaked at ~380 nm. In further experiments, Martini et al. (2009) investigated the OSL spectrum at ~380 nm for different stimulation times. Fig. 4 shows the OSL emission spectra for a synthetic quartz collected in sequential time intervals of 40 s, following irradiation and without any preheat. The shape of the spectra suggested that this emission band was composite but the OSL signal was not strong enough to perform further analysis. They also found a small shift in wavelength, with the longer decay time being associated with shorter emission wavelength. However, it was not clear whether or not this was related to the electrons giving rise to the slow OSL component recombining at a slightly different set of recombination centres.

Figure 4 (from Martini et al., 2009) spectra obtained under optical stimulation in time intervals (1) 5-45 s, (2) 45-85 s, (3) 85-125 s, without stimulation, (4) 125-165 s, and (5) 165-205 s). (a) The data as collected, and (b) after normalisation and offset for (1), (2), (4) and (5). The energy scale shown corresponds to 443 to 310 nm.

Recently, Lomax et al. (2015) have measured both TL and OSL emission spectra on the same samples of sedimentary quartz. TL spectra were obtained for both naturally irradiated and laboratory irradiated grains, the latter enabling the 110°C peak to be measured. For one sample the emission from this peak had maxima at ~ 380, 480 and 620 nm, in agreement with the wavelength peaks presented in the summary by Krbetschek et al. (1997). For that sample, the 280-320°C TL emission is dominated by orange-red emission at ~620 nm, though measurements on another sample show ~480 nm emission to be dominant.

The first sample was optically stimulated using green LEDs (525±20 nm) at 25°C, 125°C, 165°C and 185°C and the measurements were made on naturally irradiated quartz that had been heated to 240°C for 10 s prior to the measurement, as would be performed in a dating run. The OSL emission spectra in Fig. 5a have been corrected for detection efficiency.

Figure 5 (from Lomax et al., 2015) OSL spectra obtained during optical stimulation at four different temperatures (a) corrected for efficiency of detector and (b) data from (a) normalised to maximum of 1. The wavelength scale shown corresponds to 4.13 eV to 2.58 eV.

In Fig. 5a it can be seen that the spectra become less bright when the optical stimulation temperature is increased, an effect which can be explained by thermal quenching of the luminescence centre (Wintle, 1975; see section 7a). In Fig. 5b the spectra have been normalised to a maximum value of 1 to enable better comparisons to be made. Here it can be seen that the peak emission occurs at the same wavelength, ~360 nm, irrespective of the stimulation temperature. This is similar to the ~365 nm peak emission reported by Huntley et al. (1991).

The importance of the measurements of Lomax et al. (2015) relates to an early discussion of whether there is a shift in wavelength of the TL emission as a function of temperature. Franklin et al. (1995) observed a shift of wavelength from 376 nm for the 110°C TL peak to 430 nm for the 325°C TL peak. They concluded that a particular centre (H_3O_4) was responsible for this emission and that the temperature dependence could be explained by a distortion of the quartz lattice (Franklin et al., 1995). They also assumed that the OSL emission at 22°C (Huntley et al., 1991) was derived from the same centre. Itoh et al. (2002) argued that the measured shift was not

likely on theoretical grounds, and thus concluded that different luminescence centres were used by different TL traps. The finding that the OSL spectral peak does not change with temperature from 25 to 185°C (Lomax et al., 2015) does not support the proposal of Franklin et al. (1995).

b. RL and TL emission

The complexity of the luminescence spectrum is better observed by measurement of the radioluminescence, i.e. the luminescence observed during irradiation. The advantage of using RL is that whole spectral range can be observed, not just that part that is away from the stimulating wavelengths, as in the case of OSL. In addition, the RL intensity is much higher than that of OSL. RL spectra have been obtained on both natural and synthetic quartz, the latter being grown in the laboratory. RL emission spectra were used by Schilles et al. (2001) as a means of investigating the sensitivity changes that occur in sedimentary quartz as a result of heating the quartz through the lattice phase transitions that occur at 573 and 1050˚C. However, no deconvolution of the spectra was carried out.

Martini and Galli (2007) made RL measurements using an X-ray source on synthetic quartz, for "as grown" crystals containing 1-3 ppm of alkali ions and "hydrogen-swept" crystals containing ~0.1 ppm of alkali ions (sweeping or electrodiffusion – a process in which monovalent interstitial ions are replaced by hydrogen in a process conducted at elevated temperature under external electric field). Ions such as Na^+ and Li^+ act as charge compensators when Al^{3+} substitutes for Si^{4+} in the quartz crystal lattice and their presence or absence will affect the $[AlO_4]^o$ centre (Preusser et al., 2009). The $[AlO_4]^o$ centre concentration has been linked to the violet emission at 360 nm (Martini et al., 1995; Martini et al., 2009). Martini and Galli (2007) found the unswept quartz crystal to have emission both at ~380 nm and a wide emission band at ~570 nm; the latter was missing in the swept crystal from which the alkali ions had been removed.

More recently, Martini et al. (2012a) measured the RL spectra from 220 to 800 nm for slices of a different synthetic hydrothermally-grown quartz crystal and found emission peaks in the blue (~470 nm) and violet (~360 nm) (Fig. 6). For these experiments, they changed the concentrations of alkali ions (e.g. Na^+ and Li^+) and H^+ in the quartz by electrodiffusion. This resulted in higher intensity RL signals than those obtained for unswept quartz (Martini and Galli, 2007), and they were able to

separate five Gaussian components from the energy spectrum, with the three main ones being in the UV 3.44±0.58 eV (360±60 nm), in the blue 2.86±0.46 eV (430±70 nm) and 2.53±0.46 eV (490±90 nm), and the others at 310 and 395 nm being required for improved fitting of the experimental data.

Figure 6 (from Martini et al., 2012a) RL spectra obtained during irradiation with X-rays for synthetic quartz samples in which H^+, Na^+ and Li^+ ions had been swept in.

In a second study, Martini et al. (2012b) measured the RL and TL spectra for crushed grains from the same hydrothermally-grown crystal and from a natural pegmatitic quartz. The RL spectra for the crushed grains and the slice could be deconvoluted into five components, one in the red (620 nm), two in the blue (440 and 480 nm) and two in the UV (at 310 and 360); the composite nature of the UV emission has also been observed in TL of natural quartz (Fasoli and Martini, 2016). For the synthetic quartz, the spectrum did not change with repeated RL measurements during which doses of ~10 Gy were imparted (Fig. 7b). However, the RL spectrum for the natural quartz changed drastically with each measurement, the blue band at ~480 nm increasing monotonically (Fig. 7a). This 480 nm emission had previously been recorded in the 110°C TL peak (Martini et al., 1995).

Figure 7 (from Martini et al., 2012b) Repeated RL spectra obtained under X-rays with a dose of 10 Gy being given in each run (a) natural quartz, (b) synthetic quartz. The energy scale shown corresponds to 827 nm to 248 nm.

RL spectra have also been obtained on commercially-available quartz heated to temperatures between 500 and 1,000˚C (Pagonis et al., 2014). These experiments resulted in strong luminescence emissions and when deconvolution was carried out, seven Gaussian peaks were needed to fit the energy spectrum, with wavelengths centred at 635, 490, 440, 395, 360, 330 and 315 nm (Fig. 8).

Figure 8 (from Pagonis et al., 2014) Deconvolution of RL spectra into 7 Gaussian components for a sample of commercially-available natural quartz previously heated to 700°C. The energy scale shown corresponds to 708 nm to 248 nm.

Since the same emission bands are found in both natural and synthetic quartz (Martini et al., 2012b), and in the latter intensities can be changed by electrodiffusion (Martini et al., 2012a), Martini et al. (2014) concluded that the Al centres are linked to the luminescence properties of natural quartz as previously hypothesised (Martini et al., 1995, 2009). However, conclusive assignment of individual emission bands to specific defects has not yet been possible (Martini et al., 2014).

c. Ionoluminescence emission

Luminescence is also obtained when quartz is implanted with ions, resulting in ionoluminescence (IL), alternately known as ion beam luminescence (IBL). Using 0.95 MeV protons for excitation allows the full UV-IR (6.2-1.1 eV) emission spectrum to be observed. King et al. (2011) used hydrogen ions, viz. 0.95 MeV protons, from a van de Graaff particle accelerator to study samples of sedimentary quartz (including Risø calibration quartz), as well as a crystal of natural hydrothermal quartz. The 0.95 MeV protons deposit their energy to a depth of ~ 11 μm. The initial IL spectra for these samples, obtained for an irradiation time of 190 s during which time a dose of ~ $4x10^7$ Gy was delivered, were found to have two broad emission bands (Fig. 9), viz. 1.8-1.9 eV (653-689 nm) and 3.2-3.6 eV (344-387 nm).

Figure 9 (from King et al., 2011) Ionoluminesence spectra from four natural quartz samples (A, B, C, D) measured at room temperature for 190 s when stimulated with 0.95 MeV protons. A is calibration quartz.

Comparison with the energy window (3.4-3.6 eV; 364-387 nm) of the 7.5 mm thick Hoya U340 filter used for OSL dating suggests that only the tail of the UV-violet emission would be passed. The same conclusion would be drawn if single grain OSL measurements made with laser stimulation at 532 nm used a 2.5 mm thick Hoya U340 (Ballarini et al., 2005). When the spectrum for the calibration quartz (A in Fig. 9) was deconvoluted into Gaussian components, three major components were found, 3.66±0.17 eV (UV; 340±20 nm), 3.34±0.18 eV (UV-violet; 370±20 nm) and 2.97±0.29 eV (violet; 420±40 nm); the red emission in Fig. 9 could be split into two smaller components at 1.84±0.14 eV (red; 670±20 nm) and 2.23±0.16 eV (orange; 560±20 nm (King et al., 2011).

When the ion implantation run was repeated, and thus the dose delivered was increased, the red emission increased, whilst the UV-violet emission decreased. This effect was permanent, at least on the scale of a few days. King et al. (2011) considered the interplay of these two emission bands with increasing dose in the context of the existing models for luminescence production in quartz and concluded that the decrease in UV-violet emission was consistent with irradiation-induced migration of charge compensating alkali ions (M) from [AlO_4/M] centres. For all the samples, they found a power-law relationship between the ratio of the emission bands and the dose delivered, as exemplified in Fig. 10 for a sample of Risø calibration quartz.

Figure 10 (from King et al., 2011) Red and UV/violet ionoluminescence signals (and their ratio) as a function of dose delivered as measured for calibration quartz by repeated runs in which doses of ~4 10^7 Gy are delivered.

They concluded that this dose dependence could account for the different OSL sensitivities found for quartz, with low sensitivities likely to be found for quartz derived from granite bedrock with high radioactivity; this would be the result of the decreased UV-violet emission caused by the radiation received in the recent geological history of the quartz.

d. Summary

In recent years, advances in spectral measurements of OSL have been made, but there is still need for further research in order to assign particular defects to the different emission bands. In addition, to the present day the spectral information has not been tested by means of the existing numerical models of luminescence in quartz. In addition, results from other techniques such electron spin resonance (ESR) are necessary to fully answer these questions (e.g. Toyoda, 2015 or Toyoda et al., 2016).

6. Time-resolved OSL

Besides measuring the OSL under continuous stimulation, whether as CW-OSL or LM-OSL signals, it is also possible to measure the OSL when the stimulation source is pulsed. Both during and after a short stimulation pulse, photons are recorded by the detector. The stimulation pulse is repeated many times and the signals are summed to

show the build-up of luminescence during the pulse and the decay of luminescence after it is switched off (Fig. 11). The decaying signal can be approximated by the sum of several exponential decays, each characterised by a luminescence lifetime. This results in a time-resolved OSL (TR-OSL or TRL) signal (sometimes called pulsed OSL) that provides insight into the recombination process. The first TR-OSL measurements on common sedimentary minerals were made on feldspars (Sanderson and Clark, 1994), with publications on quartz appearing in 2000, with measurements made with a laser (Bailiff, 2000) and with light-emitting diodes (Chithambo and Galloway, 2000). A comprehensive review of time-resolved luminescence of quartz has just been published (Chithambo et al., 2016) and the reader is directed to this study, where a historical overview is presented.

Figure 11 (from Pagonis et al., 2009b) Comparison of experimental data with results of simulations for time-resolved luminescence.

During OSL measurements, electrons are optically evicted from traps and reach the conduction band. From the conduction band, the electrons reach the luminescence centres, putting them in an excited state. Relaxation of the luminescence centre from its excited state to the ground state can result in the emission of a photon. The lifetimes calculated from the build-up and decay of the OSL signals are the same, about 32 μs, relating to the recombination mechanism at the luminescence centre. This process has been shown to be dependent on the temperature of stimulation (Chithambo et al., 2016). Further information on the processes involved in luminescence production can be seen by comparing TR-OSL measurements with the time-resolved optically stimulated exo-electron emission (TR-OSE) made simultaneously on sand-sized quartz grains (Tsukamoto et al., 2010; Fig. 12). The majority of the TR-OSE signal decays much faster than the TR-OSL signal with a lifetime of ~ 0.6 μs; this is related to emptying of the conduction band after optical stimulation.

Figure 12 (from Tsukamoto (2010) Time-resolved OSL (a) and OSE (b) from quartz measured at stimulation temperatures of 50, 100, 150, 200 and 250°C using pulsed LED stimulation with on-time of 50 μs and off-time of 100 μs.

Pagonis et al. (2014) have constructed a mathematical model for quartz luminescence production involving two luminescence centres and one non-radiative recombination centre. This model has been able to predict the change in apparent luminescence lifetime measured for synthetic quartz annealed to temperatures of 500˚C and above. This model was also used to predict the change of luminescence lifetime observed as the stimulation temperature is changed (Pagonis et al., 2014).

Besides studying TR-OSL in order to provide information on the processes of luminescence production, measurements of TR-OSL on sedimentary minerals can have a practical use. Using an artificial mixture of quartz and feldspar grains, Denby et al. (2006) showed that it was possible to obtain a signal from quartz with minimal contribution from feldspars. This is because the TR-OSL of feldspars is quite different, with lifetimes (~ 2 μs) being very much less than for quartz (Tsukamoto et al., 2010). This approach would be useful for quartz grains containing feldspar inclusions or in measurements of rock surfaces where mineral separation is not possible (Bailiff and Mikhailik, 2003; Sohbati et al., 2012).

7. OSL production temperature dependence

The magnitude and shape of OSL decay curves can be changed by carrying out the stimulation at different temperatures (McKeever et al., 1997; Bailey, 2001). When stimulation temperature is increased at least four processes are in operation: thermal quenching; thermal ejection of electrons from traps; thermal assistance and the sensitisation caused by transfer of holes (e.g. Bailey, 2001; Adamiec, 2005a) not dealt with here.

a. Thermal quenching

In interpreting the relationship between OSL (measured at one temperature) and TL data sets (measured over a range of temperatures), it is important to understand the behaviour of the observed luminescence centre as a function of temperature. Unlike other luminescence centres, that observed in the range 360-420 nm exhibits thermal quenching; thermal quenching is the term used to describe the loss of luminescence efficiency of the recombination (hole) centre with increasing temperature.

Thermal quenching in quartz is explained in terms of the Mott-Seitz model (Bøtter-Jensen et al., 2003 pp. 44-47). In this model, electrons released from traps into the conduction band recombine with holes trapped at recombination centres in the

forbidden energy gap. A configuration coordinate diagram (Fig. 16a) is used to represent the potential energy of the ground and excited state of a luminescence centre. In centres for which the two potentials cross over, as the temperature is raised the likelihood of non-radiative transition from one state to the other increases; in this model, all recombination transitions occur within the recombination centre. The non-radiative recombination occurs through the emission of phonons, i.e. quasi-particles representing crystal lattice vibrations. Increased likelihood of non-radiative recombination results in a decrease of observed luminescence efficiency.

The 365 nm emission of the 325°C TL peak has been shown to exhibit thermal quenching (Wintle, 1975; Spooner, 1994; Petrov and Bailiff, 1995, 1997; Nanjundaswamy et al., 2002; Kitis et al., 2003). For TL and RL emission observed with a spectrometer, Schilles et al. (2001) found the energy of the thermal quenching process to be 0.65 eV. For blue emission at 470 nm, thermal quenching occurred at higher temperatures and had a higher energy, 1.32 eV. Thermal quenching has also been reported for TL emission at a wavelength of 600±40 nm for both the rapidly bleached TL peak at 325°C and the slowly bleaching peak at 375°C (Spooner and Franklin, 2002). For red emission, they found that the energy relating to thermal quenching (0.14±0.02 eV) is about a quarter that reported by others for the UV emission (Bøtter-Jensen et al., 2003, pp. 177-179).

Numerical simulation of the effect of thermal quenching of UV emission on TL glow curves has been carried out (Subedi et al., 2010) and comparisons made with experimental data for nine samples of quartz (Subedi et al., 2011, 2012). When the heating rate is changed, the temperature at which the maximum TL emission occurs varies with temperature (Chen and Pagonis, 2011, pp. 66-67), as illustrated by the work of Spooner (1994) for the “325°C” TL peak. The integrated light sum for this peak should remain constant since the number of electrons released is irrespective of the heating rate. However, the light sum will be affected by thermal quenching as the peak emission temperature is raised. This was observed by Subedi et al. (2011, 2012) for quartz samples having several different TL peaks. The decrease in luminescence efficiency with increasing temperature is shown as n(T) for the “110°C” TL peak in Fig. 13 where the results are compared with parameters of Petrov and Bailiff (1997) W = 0.79 eV and C = 4.1×10^{10}, where C is a numerical parameter (Bøtter-Jensen et al., 2003, p. 45). In Fig. 14 results for this peak and two higher temperature peaks are

given and compared with the parameters of Wintle (1975), W = 0.65 eV and C = 2.4 x10^7.

Figure 13 (from Subedi et al., 2011) Luminescence efficiency as a function of temperature obtained by measurement of the "110°C" peak for different heating rates, and calculated using the parameters of Petrov and Bailiff (1997).

Figure 14 (from Subedi et al., 2011) Luminescence efficiency measured as for Fig. 13, but over an extended temperature region using two additional peaks. Crosses are for the 110°C peak and stars for the higher temperature peaks, and the line represents values calculated using the parameters of Wintle (1975).

Thermal quenching has also been reported for the 365 nm OSL emission (Spooner, 1994; Franklin et al., 1995; Duller et al., 1995; Huntley et al., 1996; McKeever et al., 1997; Murray and Wintle, 1998). Lomax et al. (2015) also showed thermal quenching of the OSL occurring for a range of wavelengths between 330 and 450 nm (Fig. 5a in section 5).

Optical stimulation at elevated temperatures not only resulted in a decreased OSL intensity, but also to an observed decrease in the lifetime of the time-resolved OSL (Chithambo, 2003; Ogundare and Chithambo, 2007) as illustrated in Fig. 15. Chithambo and Ogundare (2009) obtained for BDH quartz an activation energy for thermal quenching of 0.64±0.04 eV.

Figure 15 (from Chithambo, 2003) Lifetime of the time-resolved OSL measured using pulsed stimulation at 525 nm as a function of the stimulation temperature.

Pagonis et al. (2010) have recently used these experimental data, together with numerical simulations, as the basis of a new kinetic model for pulsed OSL based on the Mott-Seitz model (Fig. 16). This model incorporates the effect of thermal quenching on the lifetime of the TR-OSL signal and enables interpretation of Fig. 15.

Figure 16 (from Pagonis et al., 2010) (a) Configurational coordinate diagram outlining the Mott-Seitz mechanism in quartz. (b) Energy level diagram based on the Mott-Seitz model and related to production of TR-OSL

b. Thermal assistance

Electrons are thermally ejected from the trap of the fast OSL component as temperatures are increased close to 300˚C, resulting in a reduction in the magnitude of the signal. At lower stimulation temperatures, when no thermal loss occurs, the magnitude of the signal reduction is affected predominantly by thermal quenching, as discussed in previous section, with lower signals occurring at higher temperatures. The OSL signal will also decrease with increasing temperature if there is a contribution to the observed luminescence signal from shallower traps from which electrons are either optically or thermally ejected.

The presence of shallow traps influences the shape of LM-OSL curves. This was investigated by Bulur et al. (2000) and more recently, in their study of thermal activation characteristics of a geological quartz by Kiyak et al. (2008). In both studies, LM-OSL curves were measured at both room temperature and at 125°C. The main difference was related to the presence or absence of a fourth component of the OSL signal. The studies concluded that this signal is related to the optical bleaching of the 110°C TL peak. The contribution from such shallow traps is removed by a preheat ahead of optical stimulation. However, retrapping in the shallow traps may occur during optical stimulation, with instantaneous thermal stimulation resulting in a TL signal that is added to the OSL signal (Wang et al., 2015).

Even when these shallow traps are empty, the shape of the CW-OSL decay curve is affected by changing the temperature of the optical stimulation due to the phenomenon of thermal assistance (Bøtter-Jensen et al., 2003, pages 37-44, 179-180). The rate of OSL decay (ρ) during the measurement is governed by the empirical equation $\rho = \rho_0 e^{-\frac{\Delta E}{kT}}$ where ΔE is the thermal assistance activation energy (Spooner, 1994; Huntley et al., 1996; Bailey, 2001) that depends on the stimulation wavelength. Murray and Wintle (1998) determined its value for a stimulation wavelength of ~ 470 nm and found it to be of the order of 0.045 eV. This value is consistent with that found in previous studies using a range of stimulation wavelengths (Spooner, 1994; Huntley et al., 1996). Jain et al. (2005b) determined the value of ΔE for the stimulation wavelength of ~830 nm to be equal 0.41 ± 0.02 eV.

Chruścińska (2010) has modelled the dependence of the optical cross section as a function of photon energy and stimulation temperature which takes into account

electron-phonon interactions. The approach developed by Noras (1980) led to a formula that is applicable over a range of stimulation temperatures and takes the form

$$\sigma(h\nu) = \frac{\kappa}{\nu\sqrt{\pi}} \int_0^\infty \xi^{\frac{1}{2}}\, e^{-\kappa^2(\xi-(h\nu-E))^2}\, d\xi$$

and $\kappa = \left(2S\,(\hbar\omega)^2 \coth\frac{\hbar\omega}{2kT}\right)^{-\frac{1}{2}}$.

Here ν is the frequency of the stimulating photon, E is the optical depth of the trap, S is the Huang-Rhys factor, i.e. the average number of phonons taking part in the electron-photon interaction, ω is the average angular frequency of the phonons, T the absolute temperature, k is the Boltzmann constant and $\hbar$ the reduced Planck constant. The optical and thermal trap depths are related by the equation $E = E_T + S\hbar\omega$.

This is a more general, physically justified approach than that described by Spooner (1994). Chruścińska (2010) has made simulations that allowed her to predict OSL decay curve shape dependence on temperature and a varying optical stimulation spectrum. Using a model with a single optical trap with a depth E_0 = 2.0 eV she determined the shape of the OSL decay curves for optical stimulation energies 1.9 eV and 2.0 eV (Figs. 17a and 17b, respectively). One of the conclusions of the simulations was that electron-phonon interactions allow optical stimulation when the stimulation energy is less than the optical trap depth.

Figure 17 (from Chruścińska, 2010) OSL decay curves obtained at temperatures ranging from 290 to 570 K calculated using a model with a single optical trap (E_0 = 2.0 eV) and using stimulating wavelengths (hν) of (a) 1.9 eV and (b) 2.0 eV). Inset shows data normalised to the initial value.

Further computer simulations were conducted by Chruścińska and Przegiętka (2010). Optical cross sections were derived for three components of experimentally measured OSL decay curves obtained for four quartz extracts and these showed a temperature dependence similar to the simulated data. These results are consistent with the conclusion reached by Spooner (1994) that the photoeviction of an electron does not occur via an intermediate bound state. Further studies of the probabilities of excitation of electrons from each trap to the conduction band have led Chruścińska and Przegiętka (2011) to conclude that the fast and medium components are related to a single trap, but it is important to consider the effect of retrapping of electrons. This

conclusion was later reached also by Wang et al. (2015) through a series of experiments aiming at determining the source of the OSL medium component in quartz.

8. Limitations on the use of OSL for dating

From the previous sections, it can be concluded that the fast component of the OSL signal can be isolated by preheating to remove thermally unstable signals and applying methods of data analysis to separate the fast component from the slower-decaying, and thus less bleachable, OSL components. However, heating and optical stimulation have been shown to affect the magnitude of subsequent OSL measurements by changing the luminescence sensitivity (Wintle and Murray, 2006). Thus, in order to compare OSL signals resulting from natural irradiation with those produced by laboratory irradiation (as needed for dating), it is necessary to monitor sensitivity changes. This led to the development of the SAR protocol (Murray and Wintle, 2000), for which several tests of validity have been developed as reviewed by Wintle and Murray (2006).

Measurements of the trap depth and the frequency factor for first order kinetic behaviour for the fast OSL component (Singarayer and Bailey, 2003; Jain et al., 2003) have allowed calculation of its long-term thermal stability. These predict that at an ambient temperature of 20 °C the lifetime is ~300 Ma and thus the fast OSL component should be useful for dating back to at least 1 Ma. However, there is considerable evidence from studies of sedimentary sections going back to at least 130 ka that, though ages back to ~ 50 ka are in agreement with independent evidence, age underestimation may occur for samples of over ca. 70 ka (for example, Watanuki et al., 2003; Buylaert et al., 2007; Lowick et al., 2010; Timar et al., 2010). Underestimation is reported for both sand-sized quartz (e.g. Buylaert et al., 2008) and silt-sized quartz (e.g. Lowick et al., 2010). Comparisons of ages obtained on both sand-sized and silt-sized quartz from the same samples down loess sections in Romania show age underestimation compared with independent ages, with more severe underestimation for the coarser grains (Timar-Gabor et al., 2011).

Dating studies using the SAR protocol on 15 samples of loess from a section at Costineşti, Romania resulted in sets of dose response curves for 4-11 μm and 63-90 μm grains shown in Figs. 18a and 18b respectively. Dose response curves for different samples were indistinguishable, and support the concept of a standardised

dose response curve for a particular grain size (Roberts and Duller, 2004). However, the dose response curves for different grain sizes were quite different with the curves for the 4-11 μm grains showing continuous growth above 200 Gy. For doses up to 1.2 kGy, the average dose response curves for the data sets used to obtain Figs. 18a and 18b are best fitted by a function

$$I(D) = I_0 + A \cdot \left(1 - e^{-\frac{D}{D_{01}}}\right) + B \cdot \left(1 - e^{-\frac{D}{D_{02}}}\right)$$

where I(D) is the sensitivity-corrected OSL intensity as a function of dose (D), A and B are the relative intensities of the two components which are characterised by doses D_{01} and D_{02}, respectively. The curves obtained using this double saturating exponential (DSE) function are shown as continuous lines in Figs. 18c and 18d, respectively.

Figure 18 (from Timar-Gabor and Wintle, 2013) Laboratory dose response curves obtained using a SAR protocol for samples of loess from Costinești, Romania (a) for 4-11 μm grains and (b) 63-90 μm grains. (c) and (d) averaged dose response curves using data from (a) and (b) fitted with double exponential function (GC-DSE) and average values for sensitivity-corrected natural values for the same samples fitted with a single exponential function (GC-SSE).

Typically, the values for D_0 for the two saturating exponential functions when doses up to 10 kGy are given are 175±10 Gy and 1823±10 Gy for 4-11 μm grains and 55±3 Gy and 586±5 Gy for 63-90 μm grains (Timar-Gabor et al., 2012). Similar values have been obtained for the same two grain sizes from samples of Chinese loess as well as other sites in Romania when the doses used to construct the dose response curves are taken up to 5 kGy when the dose response curves appear to be fully saturated (Timar-Gabor et al., 2017). In this study, it was also noted that the maximum dose used for fitting affected the values of D_0 obtained; this finding makes the use of a calculated D_0 value unreliable as a characteristic.

Assuming that the values of D_0 are measured using doses up to 5 kGy, it is appropriate to ask whether use of the criterion of $2D_0$ as a dose limit for dating, as proposed by Wintle and Murray (2006), is meaningful. Presumably it would need to be based on the value for the component that reaches saturation first; in terms of the above example, this would be 175 Gy for 4-11 μm grains and 55 Gy for the 63-90 μm

grains. Timar-Gabor et al. (2017) have also demonstrated that both D_0 values are related to grain diameter through an inverse square root relationship. This finding casts doubt on using D_0 as a meaningful criterion for dating.

A more appropriate method of determining the limitation of dating using the SAR protocol is to use known-age samples. A useful approach has been to plot the sensitivity-corrected natural signals obtained down sections going back 130 ka as a function of expected equivalent dose. Chapot et al. (2012) demonstrated that for 35-63 μm grains from a Chinese loess section, the natural signals did not increase with expected equivalent doses beyond ~ 400 Gy. For the 63-90 μm grains from the Romanian loess section, negligible growth in signals was found for doses above ~100 Gy and for 4-11 μm grains the limiting value was ~ 200 Gy (Fig. 18c and 18d) (Timar-Gabor and Wintle, 2013). Comparisons of the natural signal data set as a function of the expected geological dose with the laboratory dose response curve show that for neither grain sizes are the responses identical. For the 4-11 μm grains, overlap occurs up to ~ 200 Gy for which an age of ~ 65 ka would be obtained at this loess section; above ~ 200 Gy, ages obtained by SAR would be underestimated. For 63-90 μm grains, the curves overlie each other up to only ~ 50 Gy (corresponding to an age of ~ 20 ka), beyond which both over- and underestimation of ages would result. Further comparisons made at other sites show that the age discrepancies are not linked to the geological origin of the sediment (e.g. Trandafir et al., 2015).

As a result of saturation of SAR dose response curves, and problems with age underestimation, other luminescence signals from quartz have been explored.

9. OSL measurements under different stimulation conditions

a. Changing the stimulation wavelength to produce VES-OSL

In their first study on using OSL for dating, Huntley et al. (1985) used green light with a wavelength of 514.5 nm (the green line of an argon ion laser). Later, after Bøtter-Jensen et al. (1999) showed that blue diodes could be used as a source of stimulating light, most measurements of quartz OSL have been made using the 470±30 nm light for stimulation. However, other wavelengths have also been explored, following measurements of stimulation spectra (see Bøtter-Jensen et al., 2003, pages 141-148) using single wavelength optical bleaching studies (e.g. Spooner, 1994), narrow band stimulation (e.g. Ditlefsen and Huntley, 1994; Huntley et al.,

1996) and continuous scanning of stimulation wavelengths (Duller and Bøtter-Jensen, 1996).

The most recent stimulation spectrum using continuously varying the stimulation wavelength from 440 to 600 nm was shown by Chruścińska (2014, 2015). The scans (VES-OSL – variable energy of stimulation OSL) were obtained using low scanning rates of 0.0055 and 0.011 nm s^{-1}. In this approach the aim is to empty electron traps while the energy of the photons of stimulating light is continuously increased. This results in a curve similar to a TL glow curve. This process may yield valuable information about the properties of the traps involved in the OSL process (Chruścińska, 2010), e.g. the width of the observed peaks may indicate the strength of coupling of a given trap with the crystal lattice. In addition, a better separation of the different electron traps may be observed than in LM-OSL or CW-OSL. Fig. 19 (Chruścińska, 2014) shows examples of VES-OSL curves.

Figure 19 (from Chruścińska, 2014) Examples of curves obtained in VES-OSL measurements at room temperature and 125°C. The scans were obtained after irradiation with 70 Gy using a scanning rate of 0.0012 eV s^{-1}. The energy scale shown corresponds to 653 nm to 451 nm.

Singarayer and Bailey (2004) measured the dependence of the optical cross sections of the fast and medium components on stimulation wavelength by measuring the OSL remaining after bleaching with light of wavelengths in the range 375-830 nm. The bleaching rates of the two components diverged as the wavelength was increased. Bailey et al. (2011) used three wavelengths (470, 525 and 550 nm) to confirm this finding and OSL decay curves were obtained for several temperatures between 140 and 250˚C. From this study, they concluded that using green light (525 nm) for stimulation at temperatures of 130 and 160˚C provides the best compromise for separation of the fast and medium components, whilst maintaining the appropriate number of components in the subsequent analysis of the decay curves. More recently, Kijek et al. (2014) have carried out stimulation at both room temperature (Fig. 20) and at 125˚C with 8 selected wavelengths from 440 to 720 nm. The effective optical cross sections (i.e. optical cross-sections that take into account that stimulating light covers a range of wavelengths rather than is of one, single wavelength) of the four

components of the OSL decay curve increase with stimulation energy, consistent with theoretical prediction (Chruścińska, 2010).

Figure 20 (from Kijek et al., 2014) Room temperature OSL decay curves normalised to the initial value when stimulation was carried out using the indicated wavelengths of stimulating light. The quartz grains extracted from a brick were irradiated in the laboratory with a dose of about 690 Gy and stored for at least a day.

b. Changing the temperature during stimulation to produce TOSL and TM-OSL

When stimulation is carried out at a given wavelength, the temperature of the readout is usually kept constant. However, changing the temperature can also provide valuable information about the electron traps in the investigated material. One type of measurement called thermo-optically stimulated luminescence (TOSL) relies on short periods of stimulation performed during heating spaced out by set intervals of time (or temperature) as first used for feldspars (see Bøtter-Jensen et al, 2003, pp. 189-193). This type of measurement has also been applied to quartz (Wang et al., 2015). By comparing the TOSL data set for a sample that had been heated to 260 °C with the corresponding TL glow curve obtained without optical stimulation, the effect of temperature on the OSL signal can be seen (Fig. 21). The results were used as evidence for retrapping in the 170 °C TL trap (Wang et al., 2015).

Figure 21 (from Wang et al., 2015) (a) TOSL curve obtained as TL glow curve with pulsed optical stimulation and TL glow curve obtained without optical stimulation, both after preheating at 260°C for 10 s; top right shows CW-OSL stimulated at 125°C with power of 1.92 mW/s for 5.8 s.

Recently, Chruścińska and Kijek (2016), suggested a slightly different approach for analysing trap parameters, measuring a thermally modulated OSL (TM-OSL). In this approach, optical stimulation is performed during the heating until traps are fully emptied. This results in an OSL glow curve in which a better separation of signals originating from various traps is seen due to their differing dependence of the optical cross-section on temperature and wavelength. Potentially this could provide a

tool for probing very deep traps without the need to heat the samples to very high temperatures.

c. Infrared stimulation

Most OSL studies have concentrated on optimising the stimulation energy in the visible part of the spectrum. However, in an early study, Bailey (1998) had shown that an infrared stimulated luminescence (IRSL) signal was observed when quartz was exposed to IR (875 nm) at 220˚C for a few thousand seconds. The IRSL decay curve matched the depletion of the fast OSL component under the same experimental conditions. At this time, Bailey (1998) considered the outcome in terms of possible IR in laboratory lighting. Subsequently, Singarayer and Bailey (2003) demonstrated that IR stimulation at 160˚C for 6,000 s bleached only the fast OSL component, and not the medium or slow components. This behaviour was explained in terms of the very small IR photoionization cross sections for the latter components (Singarayer and Bailey, 2003; Jain et al., 2003).

Reduction of the OSL signal by IR exposure for 1,500 s when quartz grains are held at 160˚C was used by Jain et al. (2005b) in order to obtain a measure of the fast component, free of any medium or slow component. The difference in the size of 0.1 s OSL signals measured both before and after the OSL exposure was used as a measure of the fast OSL. However, this type of measurement is time consuming for a single aliquot procedure because of the long IR stimulation time.

Fan et al. (2009) confirmed that the IRSL signal measured at 150˚C for 40 s (after a preheat at 260˚C to remove any isothermal TL) comes from a trap with the same thermal stability as the fast component of the OSL obtained under blue light stimulation. Fig. 22 shows a set of pulse-annealing curves of the IRSL and OSL signals. Using heat-treated quartz, they demonstrated the viability of a single aliquot dating procedure, but concluded that it would only be of use for samples with a high luminescence sensitivity.

Figure 22 (from Fan et al., 2009) a) and b) show pulse annealing curves of the 40 s IRSL and 0.1 s OSL signals. The IRSL was recorded at 150°C. The plots c) and d) show reduction of the respective signal per °C.

Bailey (2010) also measured the IRSL at 160˚C to sample the fast OSL component, but used a relatively short IR stimulation time of 40 s and confirmed that the source of the IRSL was the same as the fast OSL component. Bailey (2010) also developed and tested on a suite of sedimentary samples a SAR procedure using a 40 s IRSL measurement incorporated within the more usual SAR sequence. However, the similarity of the results obtained when using the IRSL signal and when using the integrated CW-OSL signal or using the fast component from LM-OSL measurements, did not suggest the method had any advantage and, in any case, the IRSL methods would be limited to quartz with high sensitivity and no feldspar contamination.

10. Thermally transferred OSL

Thermally-transferred OSL (TT-OSL) is observed (e.g. at 125°C) at the end of a sequence which involves giving a dose, followed by a preheat (e.g. 10 s at 260°C) to thermally empty shallow TL traps (e.g. at 160, 220 and 280°C), an optical stimulation at 125°C and a subsequent preheat (e.g. in the range 160-300°C); the OSL signal recorded in the next measurement is referred to as the TT-OSL. As seen in Fig. 23, the initial part of the TT-OSL decay curve is several orders of magnitude smaller than the preceding OSL measurement resulting from the same dose and made under the same conditions; however, the photoionisation cross-sections are the same (Duller and Wintle, 2012; Koul et al., 2014) and thus it is concluded that the immediate source of both signals is the 325°C TL trap. In the case of the TT-OSL, the electrons have been thermally transferred from a deeper trap, e.g. the 375°C TL trap (Adamiec et al., 2010), to the 325°C TL trap. The production of TT-OSL has been modelled by Pagonis et al. (2008, 2009c).

Figure 23 (from Wang et al., 2006a) OSL signal measured at 125°C as a function of stimulation time, following a natural radiation dose of ~200 Gy. After 200 s of optical stimulation, the aliquot is heated at 260°C for 10 s and the optical stimulation at 125°C recommences and results in the TT-OSL signal. The inset shows the TT-OSL signal on a linear scale, following subtraction of the background signal from slow OSL components.

Duller and Wintle (2012) provided a review of TT-OSL measurement procedures and the use of the TT-OSL signal for dating based on the laboratory

protocol of Wang et al. (2006a, 2007). The measured TT-OSL signal can be separated into two components, the recuperated OSL (ReOSL) and a basic-transferred OSL (BT-OSL) (Wang et al., 2006a). Adamiec et al. (2010) estimated the lifetime at 10°C to be ~4.5 Ma for the ReOSL signal which would result in 10% age underestimation for a sample of 1 Ma. For the BT-OSL, the equivalent lifetime was ~48,000 Ma. Shen et al. (2011) also determined the trap depth on three samples of sedimentary quartz and concluded that the main TT-OSL signals (ReOSL) was even less stable, ~240 ka at 10°C indicating that a double transfer mechanism may contribute some charge to the TT-OSL in the protocol they used. Thiel et al. (2012) determined the TT-OSL life-time on the basis of geological data to be 0.7 Ma at 19°C in coastal deposits from Tunisia. On the other hand Liu et al. (2016) found a TT-OSL life time of 280 ka in lacustrine deposits in northern China.

However, when reviewing previously published dating results, Arnold et al. (2015) reported correspondence of the TT-OSL ages with independent (or semi-independent) age controls (Fig. 24).

Figure 24 (from Arnold et al., 2015) TT-OSL ages versus independent age estimates or semi-independent age estimates obtained using conventional luminescence dating methods (TL, fading-corrected IRSL, OSL).

The oldest sample from an archaeological site in South Africa gave an age of 1.1 Ma, in agreement with ages obtained using U-Pb and palaeomagnetic measurements (Pickering et al., 2013). This study used the ReOSL signal measured using a protocol based on that of Adamiec et al. (2010), in which the luminescence sensitivity monitor is provided by the OSL response to a very low test dose; this has the advantage of being the luminescence signal that is closest to the TT-OSL signal and is less likely to have been affected by the additional preheating that would have been required if a TT-OSL signal was being used as the monitor. This protocol was also used to obtain ages back to 400 ka for three other coastal sands on the South African coast (Jacobs et al., 2011); for these samples the BT-OSL and ReOSL equivalent doses (D_e) obtained for each aliquot were in agreement (Fig. 25). This implies that the lifetime of the ReOSL signal is adequate for dating back to at least 400 ka. In relation to this it has to be stated that the lifetime calculated using E and s

parameters of traps are extremely sensitive to the value of E, therefore it may be easy to under or overestimate the lifetime.

Figure 25 (from Jacobs et al., 2011) BT-OSL D_e values plotted as a function of their ReOSL D_e values for Middle Pleistocene sands from the southern South Africa coast.

Other TT-OSL studies of known age samples have been less successful, perhaps because it has not been possible to develop a broadly applicable protocol analogous to the SAR protocol for OSL. Several modifications of the protocol have been tested on 20-41 μm quartz grains from a single sample by Hernandez et al. (2012); they concluded that only samples that did not show significant changes between the first and subsequent cycles and/or did not need high temperature treatment at the end of each cycle were suitable for TT-OSL dating. Chapot et al. (2016) applied a slightly different TT-OSL protocol to 4-11 μm quartz grains from a sedimentary sequence with an independent time scale reaching back 1 million years. The protocol involved heating to 260°C nine times after measurement of the TT-OSL signal and giving a test dose of 165 Gy and using the subsequent TT-OSL signal for normalisation. This led to severely underestimated ages for the loess section at Luochuan (Fig. 26) obtained either using the SAR protocol or combining the natural (L/T) and dose rate for each sample. A similar approach had been applied to the testing of OSL signals (Chapot et al., 2012). Chapot et al. (2016) concluded that the source trap for the TT-OSL had insufficient thermal stability for dating beyond 50 ka, having a lifetime at 10°C of ~174 ka. However, in a study of single sand-sized grains of quartz from Atapuerca, Spain, Arnold et al. (2015) used a similar protocol to that of Chapot et al. (2016) and obtained ages between ~240 and ~930 ka that were in agreement with the independent chronology. Chapot et al. (2014) also investigated giving the large laboratory doses required for dating back to a million years as a series of doses interspersed by heating steps, as had previously been suggested by Wang et al. (2006b). They found that this approach was compromised by the thermal treatments causing sensitivity changes.

Figure 26 (from Chapot et al., 2016) TT-OSL ages obtained with a SAR protocol plotted against independently determined ages for the loess section at Luochuan.

It is still not possible to state definitively how reliable TT-OSL dating is and it needs to be stressed that a multitude of protocols is being used. From the results summarised in this review, it appears that major differences exist in the signals used for normalisation, grain size, the sensitivity of the traps to the temperatures used during the thermal treatments in the protocol; the variations in behaviour probably relate to the different geological origins of the quartz at different sites. This makes it even more difficult to directly compare the results obtained by various workers.

11. Other luminescence (and related) signals

a. Isothermal TL

The 325°C TL peak, or at least part of it, has been related to the fast component of the OSL (Spooner, 1994; Kaylor et al., 1995; Wintle and Murray, 1997; Spooner and Questiaux, 2000; Kitis et al., 2010b; Oniya et al., 2012). This relationship has led to the study of the isothermal TL signal (ITL).

Jain et al. (2007) investigated the thermal stability, optical bleachability and dose response curves for the ITL signal at 310˚C from a sample of sedimentary quartz. This study followed suggestions that the ITL signal could be used as a possible dating tool (Jain et al., 2005a, 2007; Choi et al., 2006). An advantage of using ITL rather than OSL signals has been shown to be the much higher dose saturation level of the former (Jain et al., 2005a; Choi et al., 2006; Buylaert et al., 2006; Huot et al., 2006). However, the protocol suggested by Choi et al. (2006) was later found to result in overestimation of the equivalent dose when compared with OSL measurements (Buylaert et al., 2006; Huot et al., 2006). It was concluded that the overestimation was the result of sensitivity change occurring during measurement of the natural ITL signal; this change could not be monitored as is done for OSL signals in the SAR protocol. Vandenberghe et al. (2009) developed a new protocol in which sensitivity change was forced by a preheat ahead of the ITL measurement, which was carried out at a lower temperature. By modelling the SAR OSL and SAR ITL protocols using the model and parameters of Pagonis et al. (2008), Pagonis et al. (2011) concluded that the SAR ITL protocol is more sensitive to the choice of experimental conditions and that the sensitivity changes are more complex for the ITL signals and cannot be corrected for by a SAR procedure.

Isothermal storage experiments suggested that the experimentally measured TL peak seen at 325 ˚C was made up of two peaks, the lower of which is sensitive to

blue light and is related to the OSL signal (Wintle and Murray, 1997). Its higher temperature part is more thermally stable, but is not removed by prolonged blue light stimulation. However, it is reduced to much lower levels by exposure to an artificial light source containing shorter wavelength light, as shown when the light source was a solar simulator (Jain, 2009). In that study, it was hypothesized that the traps related to the second TL peak saturate at higher doses than the traps related to OSL and the electrons in them can be reduced only by photons with higher energy than 470 nm as used for OSL measurements. This approach has been explored in section 11c.

b. Slowly decaying OSL signals

The luminescence signals discussed so far have been related to the 325˚C TL peak. Deeper traps contributing to slower OSL components have also been explored. One of the slow components, S3 of Singarayer and Bailey (2003) and S4 of Jain et al. (2003), observed using blue light stimulation was found to saturate at much higher doses than the fast OSL component in the same sample. Although the signal is only slowly bleached by blue light, it is bleached by daylight on a time scale that would make it useful for dating (Singarayer et al., 2005). Also, this signal appears to be derived from a thermally stable trap, only being reduced by heating above 600˚C (Bailey, 2000). However, its proposed use for dating using a SAR protocol (Singarayer et al., 2000) is compromised by sensitivity change.

c. Violet stimulated luminescence

Violet stimulated luminescence of quartz was examined by Godfrey-Smith et al. (1988) using the 413 nm line of a krypton laser, however they did not attempt to determine an equivalent dose using this signal. (They commented that the surface of an aluminium substrate may produce intense luminescence under such short wavelengths and suggested using other materials like stainless steel, rhodium or gold plated discs for mounting grains.)

Jain (2009) investigated the potential of a violet light source for optical stimulation using a laser diode emitting at 405 nm (3.06 eV) to produce violet stimulated luminescence (VSL). By comparing the depletion of the isothermal TL signal measured at 310˚C caused by exposure to both blue and violet light, Jain (2009) concluded that the violet light stimulates electrons from traps that are unable to be stimulated by blue light. Construction of dose response curves (after removal of the

blue OSL) showed the continued growth of the VSL for doses up to ~1 kGy, compared with only ~ 100 Gy for the OSL from the same grains.

Hernandez and Mercier (2015) has also investigated the post-blue VSL signal and compared it with other luminescence signals from the same quartz. The maximum intensity of this signal is about a tenth of the initial OSL (dominated by the fast component), but is much brighter than the TT-OSL. By observing the TL remaining after the post-blue VSL measurement, they concluded that the violet light stimulation caused a 20% reduction in the TL signal between 370 and 390°C. This confirms that a trap deeper than that used in OSL gives rise to the post-blue VSL.

Ankjærgaard et al. (2013) investigated the post-blue VSL signal as a dating tool and obtained ages up to 330 ka. To test whether this signal can be used for older samples, Ankjærgaard et al. (2015) measured the VSL of quartz extracted from palaeosols between basalt flows that had potassium-argon ages from 1.58 and 0.74 Ma; no ages over 0.58 Ma were obtained. Ankjærgaard et al. (2015) concluded that either there had been some thermal resetting of the VSL signal from the sedimentary quartz or the SAR protocol applied was inappropriate. Using loess from Luochuan, Ankjærgaard et al. (2016) concluded that a SAR procedure could not be developed since sensitivity changes could not be monitored in an appropriate manner. However, a multiple-aliquot additive dose method was applied and the ages obtained back to 600 ka were in agreement with independent chronological information.

d. Thermally-assisted OSL

The existence of very deep traps (VDT), defined as those that correspond to TL glow peaks which have their peak maximum temperature above 500°C, has been reported by Kitis et al. (2010a). These cannot be monitored directly by optical stimulation as they occur in a region where black-body radiation is high and where the UV emitting luminescence centre is severely affected by thermal quenching. However, signal from these traps can be measured using a combination of optical and thermal stimulation at temperatures below 500°C; this signal is termed thermally-assisted OSL (TA-OSL) (Polymeris et al., 2015).

Measurements of natural TA-OSL signals were made on additional sedimentary quartz using OSL stimulation temperatures ranging from 75 to 260°C (Polymeris et al., 2015). For temperatures from 75 to 125°C the TA-OSL signals were low, but were substantially higher for temperatures between 150 and 260°C (Fig. 27).

Analysis of the decay curves showed that the TA-OSL reach a maximum value at 180°C; this demonstrates the importance of a trap at about 180°C that is able to retrap electron released from the VDT. A theoretical treatment of TA-OSL in quartz has been given by Polymeris (2016). This has the potential to provide a new method of dating provided that an appropriate protocol can be established.

Figure 27 (from Polymeris et al., 2015) Natural TA-OSL curves recorded at temperatures ranging between 75°C up to 260°C.

e. Exo-electron emission

Both TL and OSL signals are the result of the release of electrons into the conduction band and their recombination at luminescence centres. Thus, changes in measured TL or OSL signals cannot be related directly to changes in the numbers of electrons released or to changes in the numbers of recombination centres. However, there is one way in which the two halves of the process of TL and OSL production can be observed separately. Once electrons are in the conduction band and are free to move within the crystal, a proportion can be released from the surface layer (~several nm) of the crystal and results in a phenomenon known as exo-electron emission.

Optically stimulated exo-electron emission (OSE) has been measured from sedimentary quartz grains (Ankjærgaard et al., 2008) using a Geiger-Müller detector filled with argon (Ankjærgaard et al., 2006); measurement of the OSL can be made simultaneously. OSE has been used to determine an equivalent dose (Ankjærgaard et al., 2009). Good agreement between the experimental OSE data and theoretical predictions was found by Pagonis et al. (2009). The lifetimes of OSE and OSL signals have been measured using pulsed optical stimulation (Tsukamoto et al., 2010). The time-resolved OSE (TR-OSE) signals decayed much faster than the TR-OSL signals, leading to the conclusion that the lifetime of the emission of the OSL signal is related to the recombination centre. Further study of OSE may lead to a new dating procedure that is free from effects such as sensitivity change, related to the luminescence centres.

12. Summary

Over the past decade, OSL signals have been used increasingly to provide chronological information for sedimentary deposits. Such use of luminescence signals

requires knowledge of fundamental properties such as trap depths (in order to predict the likely thermal stability of the signal since the grains were deposited) and photoionisation cross-sections for the incident photon energies in sunlight (in order to predict the bleachability of the signal) and for the photons from the stimulation light source and the effect of holding at a fixed temperature during stimulation (in order to choose the optimal stimulation wavelength). In addition, knowledge is required concerning the luminescence centres (in order to select appropriate optical filters for observation of the OSL signal). The parameters measured for these properties are then combined in energy band models that enable prediction of signals measured in the laboratory. Such models are of particular importance when experimental protocols are developed for obtaining the equivalent doses that is used in the age calculation.

In this paper, we have reviewed, within the framework of the energy band model of Bailey (2001), the various techniques used to provide information on the fast component of the OSL signal that is used for dating and on other luminescence signals from quartz that have been proposed as of use to extend the period of time that luminescence dating can be used. Since the review by Wintle and Murray (2006), different methods of measurement, such as LM-OSL, HM-OSL and RSP-OSL, have been further investigated and mathematical analyses applied. The general conclusion is that CW-OSL measurements provide the best data sets for separation of the fast component.

In the last decade, OSL emission spectra have been obtained for both natural sedimentary quartz (Lomax et al., 2015) using stimulation at 460 nm and synthetic quartz (Martini et al., 2009) using stimulation at 525 nm, though the signal was not strong enough to apply spectral analysis. To increase the luminescence signal size and spectral range, RL spectra have been recorded under stimulation by X-rays for both synthetic (Martini et al., 2012b) and natural quartz (Martini et al., 2012b; Pagonis et al., 2014) which show the complexity of emission from 2.0 to 4.5 eV.

In the last three years, a new stimulation method, VES-OSL, has been developed in which the wavelength is continuously decreased from 800 to 400 nm whilst maintaining a fixed width of stimulation band (Chruścińska, 2014, 2015). This technique has the potential of being another tool for investigating the trap structure in quartz and other phosphors.

Since Duller and Wintle (2012) reviewed the measurement of TT-OSL signals from quartz, conflicting results have been obtained on known age samples, with some

being in agreement with known ages (e.g. Pickering et al., 2013) and others showing strong age underestimation (e.g. Chapot et al., 2016). Another signal that has been explored is the violet stimulated luminescence (VSL) measured after blue optical stimulation (Jain, 2009; Ankjærgaard et al., 2013). Although a SAR protocol could not be developed (Ankjærgaard et al., 2015), a technique that used multiple aliquots was developed that resulted in ages back to 600 ka (Ankjærgaard et al., 2016).

In recent years another measurement technique for probing deep traps, TA-OSL, has been suggested as reviewed by Polymeris (2016), however its application for dating quartz has not been tested yet.

Thus, in conclusion, it appears that recently-developed measurement techniques have resulted in new luminescence signals and a better understanding of the processes underlying luminescence production in quartz which in turn provides greater support for the current dating techniques. However, it must always be remembered that when a sample aliquot of a few mg is used, it is made up of several hundred grains. Studies have shown that the individual grains show a range of OSL behaviour, for example with regard to thermal sensitisation (Adamiec, 2000b), decay curve shape (Adamiec, 2005b), intensity (Arnold and Roberts, 2011), different ratios of fast and medium components (Bulur et al., 2002; Feathers and Pagonis, 2015) and dose response curves (Jacobs et al., 2003). Thus, when analysing and correlating different signals recorded for multi-grain aliquot there is a danger that different signals originate from different grains making definitive conclusions regarding the interrelation of those signals difficult.

13. Acknowledgements

We are very grateful to Dr Alicja Chruścińska, Dr Mayank Jain and Prof. Jakob Wallinga for constructive comments that helped to improve the paper.

References

Adamiec, G., 2000a. Aspects of pre-dose and other luminescence phenomena in quartz absorbed dose estimation. Unpublished D.Phil. thesis, Oxford University.

Adamiec, G., 2000b Variations in luminescence properties and pre-dose sensitisation of single quartz grains. Radiation Measurements 32, 427-432.

Adamiec, G., 2005a. Investigation of a numerical model of the predose mechanism in quartz. Radiation Measurements 39, 175-189.

Adamiec, G., 2005b. OSL decay curves – relationship between single- and multiple grain aliquots. Radiation Measurements 39, 63-75.

Adamiec, G., Duller, G.A.T., Roberts, H.M., Wintle, A.G., 2010. Improving the TT-OSL SAR protocol through source trap characterisation. Radiation Measurements 45, 768-777.

Aitken, M.J., Xie, J., 1992. Optical dating using infrared diodes: young samples. Quaternary Science Reviews 11, 147-152.

Ankjærgaard, C., Jain, M., 2010. Optically stimulated phosphorescence in quartz over the millisecond to second time scale: insights into the role of shallow traps in delaying luminescent recombination. Journal of Physics D: Applied Physics 43, 255502 (12 pp).

Ankjærgaard, C., Murray, A.S., Denby, P.M., Bøtter-Jensen, L., 2006. Measurement of optically and thermally stimulated electron emission from natural minerals. Radiation Measurements 41, 780-786.

Ankjærgaard, C., Murray, A.S., Denby, P.M., Jain, M., 2009. Using optically stimulated electrons from quartz for the estimation of natural doses. Radiation Measurements 44, 232-238.

Ankjærgaard, C., Denby, P.M., Murray, A.S., Jain, M., 2008. Charge movement in grains of quartz studies using exo-electron emission. Radiation Measurements 43, 273-277.

Ankjærgaard, C., Jain, M., Hansen, P.C., Nielsen, H.B., 2010. Towards multi-exponential analysis in optically stimulated luminescence. Journal of Physics D: Applied Physics 43, 195501 (14 pp).

Ankjærgaard, C., Jain, M., Wallinga, J., 2013. Towards dating Quaternary sediments using the quartz Violet Stimulated Luminescence (VSL) signal. Quaternary Geochronology 18, 99-109.

Ankjærgaard, C., Guralnik, B., Porat, N., Heimann, A., Jain, M., Wallinga, M., 2015. Violet stimulated luminescence: geo- or thermochronometer? Radiation Measurements 81, 78-84.

Ankjærgaard, C., Guralnik, B., Buylaert, J.-P., Reimann, T., Yi, S.W., Wallinga, J., 2016. Violet stimulated luminescence dating of quartz from Luochuan (Chinese loess plateau): Agreement with independent chronology up to ~ 600 ka. Quaternary Geochronology 34, 33-46.

Arnold, L.J., Roberts, R.G., 2011. Paper I – optically stimulated luminescence (OSL) dating of perennially frozen deposits in north-central Siberia: OSL characteristics of quartz grains and methodological considerations regarding their suitability for dating. Boreas 40, 389-416.

Arnold, L.J., Demuro, M., Parés, J.M., Pérez-González, A., Arsuaga, J.L., Bermúdez de Castro, J.M., Carbonell, E., 2015. Evaluating the suitability of extended-range luminescence dating techniques over early and Middle Pleistocene timescales: Published data sets and case studies from Atapuerca, Spain. Quaternary International 389, 16-190.

Bailey, R.M., 1997. Optical detrapping of charge from the 110°C quartz TL region. Ancient TL 15, 7-10.

Bailey, R.M., 1998. Depletion of the quartz OSL signal using low photon energy stimulation. Ancient TL 16, 33-36.

Bailey, R.M., 2000. The slow component of quartz optically stimulated luminescence. Radiation Measurements 32, 233-246.

Bailey, R.M., 2001. Towards a general kinetic model for optically and thermally stimulated luminescence of quartz. Radiation Measurements 33, 17-45.

Bailey, R.M., 2002. Simulations of variability in the luminescence characteristics of natural quartz and its implications for estimates of absorbed dose. Radiation Protection Dosimetry 100, 33-38.

Bailey, R.M., 2004. Paper I – simulation of dose absorption in quartz over geological timescales and its implications for the precision and accuracy of optical dating. Radiation Measurements 38, 299-310.

Bailey, R.M., 2010. Direct measurement of the fast component of quartz optically stimulated luminescence and implications for the accuracy of optical dating. Quaternary Geochronology 5, 559-568.

Bailey, R.M., Smith, B.J., Rhodes, E.J., 1997. Partial bleaching and the decay form characteristics of quartz OSL. Radiation Measurements 27, 123-136.

Bailey, R.M., Yukihara, E.G., McKeever, S.W.S., 2011. Separation of quartz optically stimulated luminescence components using green (525 nm) stimulation. Radiation Measurements 46, 643-648.

Bailiff, I.K., 2000. Characteristics of time-resolved luminescence in quartz. Radiation Measurements 32, 401-405.

Bailiff, I.K., Mikhailik, V.B., 2003. Spatially-resolved measurement of optically stimulated luminescence and time-resolved luminescence. Radiation Measurements 37, 151-159.

Ballarini, M., Wallinga, J., Duller, G.A.T., Brouwer, J.C., Bos, A.J.J., Van Eijk, C.W.E., 2005. Optimizing detection filters for single-grain optical dating of quartz. Radiation Measurements 40, 5-12.

Ballarini, M., Wallinga, J., Wintle, A.G., Bos, A.J.J., 2007. A modified SAR protocol for optical dating of individual grains from young quartz samples. Radiation Measurements 42, 360-369.

Banerjee, D., Bøtter-Jensen, L., Murray, A.S., 2000. Retrospective dosimetry: estimation of the dose to quartz using the single-aliquot regenerative-dose protocol. Applied Radiation and Isotopes 52, 831-844.

Bluszcz, A., Adamiec, G., 2006. Application of differential evolution to fitting OSL decay curves. Radiation Measurements 41, 886-891.

Bos, A.J.J., Wallinga, J., 2009a. Optically stimulated luminescence signals under various stimulation modes assuming first-order kinetics. Physical Review B 79, 195118.

Bos, A.J.J., Wallinga, J., 2009b. Analysis of the quartz OSL decay curve by differentiation. Radiation Measurements 44, 588-593.

Bos, A.J.J., Wallinga, J., 2012. How to visualize quartz OSL signal components. Radiation Measurements 47, 752-758.

Bøtter-Jensen, L., Duller, G.A.T., Murray, A.S., Banerjee, D., 1999. Blue light emitting diodes for optical stimulation of quartz in retrospective dosimetry and dating. Radiation Protection Dosimetry 84, 335-340.

Bøtter-Jensen, L., Bulur, E., Duller, G.A.T., Murray, A.S., 2000. Advances in luminescence instrument systems. Radiation Measurements 32, 523-528.

Bøtter-Jensen, L., McKeever, S.W.S., Wintle, A.G., 2003. Optically Stimulated Luminescence Dosimetry. Elsevier, Amsterdam (355 pp).

Bulur, E., 2000. A simple transformation for converting CW-OSL curves to LM-OSL curves. Radiation Measurements 32, 141-145.

Bulur, E., Bøtter-Jensen, L., Murray, A.S., 2000. Optically stimulated luminescence from quartz measured using the linear modulation technique. Radiation Measurements 32, 407-411.

Bulur, E., Bøtter-Jensen, L., Murray, A.S., 2001a. LM-OSL signals from some insulators: an analysis of the dependency of the detrapping probability on stimulation light intensity. Radiation Measurements 33, 715-719.

Bulur, E., Bøtter-Jensen, L., Murray, A.S., 2001b. Frequency modulated pulsed stimulation in optically stimulated luminescence. Nuclear Instruments and Methods in Physics B 179, 151-159.

Bulur, E., Duller, G.A.T., Solongo, S., Bøtter-Jensen, L., Murray, A.S., 2002. LM-OSL from single grains of quartz: a preliminary study. Radiation Measurements 35, 79-85.

Buylaert, J.-P., Murray, A.S., Huot, S., Vriend, M.G.A., Vandenberghe, D., De Corte, F., Van den haute, P., 2006. A comparison of quartz OSL and isothermal TL measurements on Chinese loess. Radiation Protection Dosimetry 119, 474-478.

Buylaert, J.P, Murray, A.S., Vanderberghe, D., Vriend, M., De Corte, F., Van den Haute, P., 2008. Optical dating of Chinese loess using sand-sized quartz: Establishing a time frame for Late Pleistocene climate changes in the western part of the Chinese Loess Plateau. Quaternary Geochronology 3, 99-113.

Buylaert, J.P, Vanderberghe, D., Murray, A.S., Huot, S., De Corte, F., Van den Haute, P., 2007. Luminescence dating of old (>70 ka) Chinese loess: A comparison of single-aliquot OSL and IRSL techniques. Quaternary Geochronology 2, 9-14.

Chapot, M.S., Roberts, H.M., Duller, G.A.T., Lai, Z.P., 2012. A comparison of natural- and laboratory-generated dose response curves for quartz optically stimulated luminescence signals from Chinese loess. Radiation Measurements 47, 1045-1052.

Chapot, M.S., Duller, G.A.T., Roberts, H.M., 2014. Assessing the impact of pulsed-irradiation procedures on the thermally transferred OSL signal in quartz. Radiation Measurements 65, 1-7.

Chapot, M.S., Roberts, H.M., Duller, G.A.T., Lai, Z.P., 2016. Natural and laboratory TT-OSL dose response curves: Testing the lifetime of the TT-OSL signal in nature. Radiation Measurements 85, 41-50.

Chen, R., Pagonis, V., 2011. Thermally and Optically Stimulated Luminescence: A Simulation Approach. Wiley, Chichester (419 pp).

Chithambo, M.L., 2003. Dependence of the thermal influence on luminescence lifetimes from quartz on the duration of optical stimulation. Radiation Measurements 37, 167-175.

Chithambo, M.L., Galloway, R.B., 2000. On luminescence lifetimes in quartz. Radiation Measurements 32, 621-626.

Chithambo, M.L., Ogundare, F.O., 2009. Luminescence lifetime components in quartz: Influence of irradiation and annealing. Radiation Measurements 44, 453-457.

Chithambo, M.L., Ankjærgaard, C., Pagonis, V., 2016. Time-resolved luminescence from quartz: An overview of contemporary developments and applications. Physica B 481, 8-18.

Choi, J.H., Murray, A.S., Cheong, C.S., Hong, H.W. 2006. Estimation of equivalent dose using quartz isothermal TL and the SAR procedure. Quaternary Geochronology 1, 101-108.

Choi, J.H., Murray, A.S., Jain, M., Cheong, C.S., Chang, H.W., 2003. Luminescence dating of well-sorted marine terrace sediments on the southeastern coast of Korea. Quaternary Science Reviews 22, 407-421.

Chruścińska, A., 2010. On some fundamental features of optically stimulated luminescence measurements. Radiation Measurements 45, 991-999.

Chruścińska, A., 2014. Experimental demonstration of the variable energy of stimulation optically stimulated luminescence (VE-OSL) method. Radiation Measurements 71, 247-250.

Chruścińska, A., 2015. Estimating the parameters of traps in quartz by the variable energy of stimulation optically stimulated luminescence (VE-OSL) method. Radiation Measurements 81, 205-211.

Chruścińska, A., Kijek, N., 2016. Thermally modulated optically stimulated luminescence (TM-OSL) as a tool of trap parameter analysis. Journal of Luminescence 174, 42-48.

Chruścińska, A., Przegiętka, K.R., 2010. The influence of electron-phonon interaction on the OSL decay curve shape. Radiation Measurements 45, 317-319.

Chruścińska, A., Przegiętka, K.R., 2011. Analysis of OSL intensity increase with temperature and its consequences for dating applications. Radiation Measurements 46, 1514-1517.

Cunningham, A.C., Wallinga, J., 2009. Optically stimulated luminescence dating of young quartz using the fast component. Radiation Measurements 44, 423-428.

Cunningham, A.C., Wallinga, J., 2010. Selection of integration time intervals for quartz OSL decay curves. Quaternary Geochronology 5, 657-666.

Denby, P.M., Bøtter-Jensen, L., Murray, A.S., Thomsen, K.J., Moska, P., 2006. Application of pulsed OSL to the separation of the luminescence components from a mixed quartz/feldspar sample. Radiation Measurements 41, 774-779.

Ditlefsen, C., Huntley, D.J., 1994. Optical excitation of trapped charges in quartz, potassium feldspars and mixed silicates: the dependence on photon energy. Radiation Measurements 23, 675-682.

Duller, G.A.T., 2008. Single-grain optical dating of Quaternary sediments; why aliquot size matters in luminescence dating. Boreas 37, 589-612.

Duller, G.A.T., Bøtter-Jensen, L., Poolton, N.R.J., 1995. Stimulation of mineral-specific luminescence from multi-mineral samples. Radiation Measurements 24, 87-93.

Duller, G.A.T., Bøtter-Jensen, L., 1996. Comparison of optically stimulated luminescence signals from quartz using different stimulation wavelengths. Radiation Measurements 26, 603-609.

Duller, G.A.T., Wintle, A.G., 2012. A review of the thermally transferred optically stimulated luminescence signal from quartz for dating sediments. Quaternary Geochronology 7, 6-20.

Fan, A., Li, S.-H., Li, B., 2009. Characteristics of quartz infrared stimulated luminescence (IRSL) at elevated temperatures. Radiation Measurements 44, 434-438.

Fasoli, M., Martini, M., 2016. The composite nature of the thermoluminescence UV emissions of quartz. Journal of Luminescence 173, 120-126.

Feathers, J.K., Pagonis, V., 2015. Dating quartz near saturation – Simulations and application at archaeological sites in South Africa and South Carolina. Quaternary Geochronology 30, 416-421.

Franklin, A.D., Prescott, J.R., Scholefield, R.B., 1995. The mechanism of thermoluminescence in an Australian sedimentary quartz. Journal of Luminescence 63, 317-326.

Friedrich, J., Kreutzer, S., Schmidt, C., 2016. Solving ordinary differential equations to understand luminescence: 'RLumModel', an advanced research tool for simulating luminescence in quartz using R. Quaternary Geochronology 35, 88-100.

Godfrey-Smith, D.I., Huntley, D.J., Chen, W.-H., 1988. Optical dating studies of quartz and feldspar sediment extracts. Quaternary Science Reviews 7, 373-380.

Heer, A.J., Adamiec, G., Moska, P., 2012. How many grains are there on a single aliquot? Ancient TL 30, 9-16.

Hernandez, M., Mercier, N., 2015. Characteristics of the post-blue VSL signal from sedimentary quartz. Radiation Measurements 78, 1-8.

Hernandez, M., Mauz, B., Mercier, N., Shen, Z., 2012. Evaluating the efficiency of TT-OSL SAR protocols. Radiation Measurements 4, 669-673**.**

Huntley, D.J., 2006. Thoughts arising from "Choi, Duller and Wintle: Analysis of quartz LM-OSL curves, Ancient TL 24, 9-20 (2006)". Ancient TL 24, 69-70.

Huntley, D.J., Godfrey-Smith, D.I., Thewalt, M.L.W., 1985. Optical dating of sediments. Nature 313, 105-107.

Huntley, D.J., Godfrey-Smith, D.I., Haskell, E.H., 1991. Light-induced emission spectra from some quartz and feldspars. Nuclear Tracks and Radiation Measurements 18, 127-131.

Huntley, D.J., Short, M.A., Dunphy, K., 1996. Deep traps in quartz and their use for optical dating. Canadian Journal of Physics 74, 81-91.

Huot, S., Buylaert, J.-P., Murray, A.S., 2006. Isothermal thermoluminescence signals from quartz. Radiation Measurements 42, 1285-1293.

Itoh, N., Stoneham, D., Stoneham, A.M., 2002. Ionic and electronic processes in quartz: Mechanisms of thermoluminescence and optically stimulated luminescence. Journal of Applied Physics 92, 5035-5044.

Jacobs, Z., Roberts, R.G., 2007. Advances in optically stimulated luminescence dating of individual grains of quartz from archaeological deposits. Evolutionary Anthropology 16, 210-223.

Jacobs, Z., Duller, G.A.T., Wintle, A.G., 2003. Optical dating of dune sand from Blombos Cave, South Africa II: single grain data. Journal of Human Evolution 44, 613-625.

Jacobs, Z., Roberts, R.G., Lachlan, T.J., Karkanas, P., Marean, C.W., Roberts, D.L., 2011. Development of the SAR TT-OSL procedure for dating Middle Pleistocene dune and shallow marine deposits along the southern Cape coast of South Africa. Quaternary Geochronology 6, 491-513.

Jain, M., 2009. Extending the dose range: Probing deep traps in quartz with 3.06 eV photons. Radiation Measurements 44, 445-452.

Jain, M., Choi, J.H., Thomas, P.J., 2008. The ultrafast OSL component in quartz: Origins and implications. Radiation Measurements 43, 709-714.

Jain, M., Lindvold, L.R., 2007. Blue light stimulation and linearly modulated stimulated luminescence. Ancient TL 25, 69-75.

Jain, M., Murray, A.S., Bøtter-Jensen, L., 2003. Characterisation of blue-light stimulated luminescence components in different quartz samples: implications for dose measurement. Radiation Measurements 37, 441-449.

Jain, M., Bøtter-Jensen, L., Murray, A.S., Denby, P.M., Tsukamoto, S., Gibling, M.R., 2005a. Revisiting TL: dose measurement beyond the OSL range using SAR. Ancient TL 23, 9-24.

Jain, M., Murray, A.S., Bøtter-Jensen, L., Wintle, A.G., 2005b. A single-aliquot regenerative-dose method based on IR (1.49 eV) bleaching of the fast OSL component in quartz. Radiation Measurements 39, 309-318.

Jain, M., Duller, G.A.T., Wintle, A.G., 2007. Dose response, thermal stability and optical bleaching of the 310°C isothermal TL signal in quartz. Radiation Measurements 42, 1285-1293.

Kaylor, R.M., Feathers, J., Hornyak, W.F., Franklin, A.D., 1995. Optically stimulated luminescence in Kalahari quartz: bleaching of the 325°C peak as the source of the luminescence. Journal of Luminescence 65, 1-6.

Kijek, N., Chruścińska, A., Przegiętka, K.R., 2014. The dependence of quartz OSL on stimulation energy. Radiation Measurements 71, 108-112.

King, G.E., Finch, A.A., Robinson, R.A.J., Hole, D.E., 2011. The problem of dating quartz 1: Spectroscopic ionoluminescence of dose dependence. Radiation Measurements 46, 1-9.

Kitis, G., Pagonis, V., 2008. Computerized curve deconvolution analysis for LM-OSL. Radiation Measurements 43, 737-741.

Kitis, G., Pagonis, V., Drupieski, C., 2003. Cooling rate effects on the thermoluminescence glow curves of Arkansas quartz. Physica Status Solidi (a) 198, 312-321.

Kitis, G., Polymeris, G.S., Kiyak, N.G., 2007. Component-resolved thermal stability and recuperation study of the LM-OSL curves of four sedimentary quartz samples. Radiation Measurements 42, 1273-1279.

Kitis, G., Kiyak, N.G., Polymeris, G.S., Pagonis, V., 2010a. Investigation of OSL signals from very deep traps in unfired and fired quartz samples. Nuclear Instruments and Methods in Physics Research B 268, 592-598.

Kitis, G., Kiyak, N., Polymeris, G.S., Tsirliganis, N.C., 2010b. The correlation of fast OSL component with TL peak at 325°C in quartz of various origins. Journal of Luminescence 130, 298-303.

Kitis, G., Polymeris, G.S., Kiyak, N.G., Pagonis, V., 2011. Preliminary results towards the equivalence of transformed continuous-wave optically stimulated luminescence (CW-OSL) and linearly-modulated (LM-OSL) signals in quartz. Geochronometria 38, 209-216.

Kiyak, N.G., Polymeris, G.S., Kitis, G., 2007. Component resolved OSL dose response and sensitization of various sedimentary quartz samples. Radiation Measurements 42, 144-155.

Kiyak, N.G., Polymeris, G.S., Kitis, G., 2008. LM-OSL thermal activation curves of quartz: Relevance to the thermal activation of the 110°C TL glow-peak. Radiation Measurements 43, 263-268.

Koul, D.K., Patil, P.G., Oniya, E.O., Polymeris, G.S., 2014. Investigating the thermally transferred optically stimulated luminescence source trap in fired geological quartz. Radiation Measurements 62, 60-70.

Krbetschek, M.R., Götze, J., Dietrich, A., Trautmann, T., 1997. Spectral information from minerals relevant for luminescence dating. Radiation Measurements 27, 695-748.

Kreutzer, S., Schmidt, C., Fuchs, M.C., Dietze, M., Fischer, M., Fuchs, M., 2012. Introducing an R package for luminescence dating analysis. Ancient TL 30, 1-8.

Lang, A., Wagner, G.A. (1997) Infrared stimulated luminescence dating of Holocene colluvial sediments using the 410 nm emission. Quaternary Science Reviews 16, 393-396.

Lapp, T., Kook, M., Murray, A.S., Thomsen, K.J., Buylaert, J.P., Jain, M., 2015. A new luminescence detection and stimulation head for the Risø TL/OSL reader. Radiation Measurements 81, 178-184.

Li, S.H., Li, B., 2006. Dose measurement using the fast component of LM-OSL signals from quartz. Radiation Measurements 41, 534-541.

Liu, J., Murray, A.S., Buylaert, J.P., Jain, M., Chen, J., Lu, Y., 2016. Stability of fine-grained TT-OSL and post-IR IRSL signals from a c. 1 Ma sequence of aeolian and lacustrine deposits from the Nihewan Basin (northern China). Boreas, 45, 703-714.

Lomax, J., Mittelstraβ, D., Kreutzer, S., Fuchs, M., 2015. OSL, TL and IRSL emission spectra of sedimentary quartz and feldspar samples. Radiation Measurements 81, 251-256.

Lowick, S.E., Preusser, F., Pini, R., Ravazzi, C., 2010. Underestimation of fine grain quartz OSL dating towards the Eemian: Comparison with palynostratigraphy from Azzano Decimo, northeastern Italy. Quaternary Geochronology 5, 583-590.

Martini, M., Paleari, A., Spinolo, G., Vedda, A., 1995. Role of $[AlO_4]^o$ centres in the 380-nm thermoluminescence of quartz. Physical Review B 52, 138-142.

Martini, M., Galli, A., 2007. Ionic mechanisms in the optically stimulated luminescence of quartz. Physica Status Solidi C: Current topics in solid state physics 4, 1000-1003.

Martini, M., Fasoli, M., Galli, A., 2009. Quartz OSL emission spectra and the role of [AlO4]° recombination centres. Radiation Measurements 44, 458-461.

Martini, M., Fasoli, M., Galli, A., Villa, I., Guibert, P., 2012a. Radioluminescence of synthetic quartz related to alkali ions. Journal of Luminescence 132, 1030-1036.

Martini, M., Fasoli, M., Villa, I., Guibert, P., 2012b. Radioluminescence of synthetic and natural quartz. Radiation Measurements 47, 846-850.

Martini, M., Fasoli, M., Villa, I., 2014. Defect studies in quartz: Composite nature of the blue and UV emissions. Nuclear Instruments and Methods in Physics Research B 327, 15-21.

McKeever, S.W.S., Bøtter-Jensen, L., Agersnap Larsen, N., Duller, G.A.T., 1997. Temperature dependence of OSL decay curves: experimental and theoretical aspects. Radiation Measurements 27, 161-170.

Murray, A.S., Wintle, A.G. 1998. Factors controlling the shape of the OSL decay curve in quartz. Radiation Measurements 29, 65-79.

Murray, A. S., Wintle, A.G., 2000. Luminescence dating of quartz using an improved single-aliquot regenerative-dose protocol. Radiation Measurements 32, 57-73.

Nanjundaswamy, R., Lepper, K., McKeever, S.W.S., 2002. Thermal quenching of thermoluminescence in natural quartz. Radiation Protection Dosimetry 100, 305-308.

Noras, J.M., 1980. Photoionisation and phonon coupling. Journal of Physics C: Solid State Physics 13, 4779-4789.

Ogundare, F.O., Chithambo, M.L., 2007. Time resolved luminescence of quartz from Nigeria. Optical Materials 29, 1844-1851.

Oniya, E.O., Polymeris, G.S., Tsirliganis, N.C., Kitis, G., 2012, Radiation dose response correlation between thermoluminescence and optically stimulated luminescence in quartz. Journal of Luminescence 132, 1720-1728.

Pagonis, V., Ankjærgaard, C., Murray, A.S., Chen, R., 2009a. Optically stimulated exoelectron emission processes in quartz: comparison of experiment and theory. Journal of Luminescence 129, 1003-1009.

Pagonis, V., Ankjærgaard, C., Murray, A.S., Jain, M., Chen, R., Lawless, J., Greilich, S., 2010. Modelling the thermal quenching mechanism in quartz based on time-resolved optically stimulated luminescence. Journal of Luminescence 130, 902-909.

Pagonis, V., Baker, A., Larsen, M., Thompson, Z., 2011. Precision and accuracy of two luminescence dating techniques for retrospective dosimetry: SAR-OSL and SAR-ITL. Nuclear Instruments and Methods in Physics Research B 269, 653-663.

Pagonis, V., Chithambo, M.L., Chen, R., Chruścińska, A., Fasoli, M., Li, S.H., Martini, M., Ramseyer, K., 2014. Thermal dependence of luminescence lifetimes and radioluminescence in quartz. Journal of Luminescence 145, 38-48.

Pagonis, V., Mian, S.M., Chithambo, M.L., Christensen, E., Barnold, C., 2009b. Experimental and modelling study of pulsed optically stimulated luminescence in quartz, marble and beta irradiated salt. Journal of Physics D. Applied Physics 42, 55407.

Pagonis, V., Wintle, A.G., Chen, R., Wang, X.L., 2008. A theoretical model for a new dating protocol for quartz based on thermally transferred OSL (TT-OSL). Radiation Measurements 43, 704-708.

Pagonis, V., Wintle, A.G., Chen R., Wang, X.L., 2009c. Simulations of thermally-transferred OSL experiments and of the ReSAR dating protocol for quartz. Radiation Measurements 44, 634-638.

Peng, J., Pagonis, V., 2016. Simulating comprehensive kinetic models for quartz luminescence using the R program KMS. Radiation Measurements 86, 63-70.

Petrov, S.A., Bailiff, I.K., 1995. Thermal quenching and the Initial Rise technique of trap depth evaluation. Journal of Luminescence 65, 289-291.

Petrov, S.A., Bailiff, I.K., 1997. Determination of trap depths associated with TL peaks in synthetic quartz (350-550 K). Radiation Measurements 27, 185-191.

Pickering, R., Jacobs, Z., Herries, A.I.R., Karkanas, P., Bar-Matthews, M., Woodhead, J.D., Kappen, P., Fisher, E., Marean, C.W., 2013. Paleoanthropologically significant South African sea caves dated to 1.1-1.0 million years using a combination of U-Pb, TT-OSL and palaeomagnetism. Quaternary Science Reviews 65, 39-52.

Polymeris, G.S., 2016. Thermally assisted OSL (TA-OSL) from various luminescence phosphors; an overview. Radiation Measurements 90, 145-152.

Polymeris, G.S., Afouxenidis, D., Tsirliganis, N.C., Kitis, G., 2009. The TL and room temperature OSL properties of the glow peak at 110°C in natural milky quartz: A case study. Radiation Measurements 44, 23-31.

Polymeris, G.S., Şahiner, E., Meriç, N., Kitis, G., 2015. Experimental features of natural thermally assisted OSL (NTA-OSL) signal in various quartz samples; preliminary results. Nuclear Instruments and Methods in Physics Research B 349, 24-30.

Poolton, N.R.J., Bøtter-Jensen, L., Andersen, C.E., Jain, M., Murray, A.S., Malins, A.E.R., Quinn, F.M., 2003. Measuring modulated luminescence using non-modulated stimulation: ramping the sample period. Radiation Measurements 37, 639-645.

Preusser, F., Chithambo, M.L., Götte, G., Martini, M., Ramseyer, K., Sendezera, E.J., Susino, G.J., Wintle, A.G., 2009. Quartz as a natural luminescence dosimeter. Earth-Science Reviews 97, 184-214.

Quinn, F., Poolton, N., Malins, A., Pantos, E., Andersen, C., Denby, P., Dhanak, V., Miller, G., 2003. The Mobile Luminescence End-Station, MoLES: A new public Facility at Daresbury Synchrotron. Journal of Synchrotron Radiation 10, 461-466.

Richter, D., Richter, A., Dornich, K., 2013. Lexsyg – a new system for luminescence research. Geochronometria 40, 220-228.

Roberts, H.M., 2008. The development and application of luminescence dating to loess deposits: a perspective on the past, present and future. Boreas 37, 483-507.

Roberts, H.M., Duller, G.A.T., 2004. Standardised growth curves for optical dating of sediment using multiple-grain aliquots. Radiation Measurements 38, 241-252.

Roberts, R.G., Jacobs, Z., Li, B., Jankowski, N.R., Cunningham, A.C., Rosenfeld, A.B., 2015. Optical dating in archaeology: thirty years in retrospect and grand challenges for the future. Journal of Archaeological Science 56, 41-60.

Sanderson, D.C.W., Clark, R.J., 1994). Pulsed photostimulated luminescence of alkali feldspars. Radiation Measurements 23, 633-639.

Schilles, T., Poolton, N.R.J., Bulur, E., Bøtter-Jensen, L., Murray, A.S., Smith, G.M., Riedi, P.C., Wagner, G.A., 2001. A multi-spectroscopic study of luminescence sensitivity changes in natural quartz induced by high-temperature annealing. Journal of Physics D: Applied Physics 34, 722-731.

Schmidt, C., Kreutzer, S., DeWitt, R., Fuchs, M., 2015. Radiofluorescence of quartz: A review. Quaternary Geochronology 26, 66-77.

Shen, Z.X., Mauz, B., Lang, A., 2011. Source-trap characterization of thermally transferred OSL in quartz. Journal of Physics D 44, 295405 (12 pp).

Singarayer, J.S., Bailey, R.M., 2003. Further investigations of the quartz optically stimulated luminescence components using linear modulation. Radiation Measurements 37, 451-458.

Singarayer, J.S., Bailey, R.M., 2004. Component-resolved bleaching spectra of quartz optically stimulated luminescence: preliminary results and implications for dating. Radiation Measurements 38, 111-118.

Singarayer, J.S., Bailey, R.M., Rhodes, E.J., 2000. Potential of the slow component of quartz OSL for age determination of sedimentary samples. Radiation Measurements 32, 873-880.

Singarayer, J.S., Bailey, R.M., Ward, S., Stokes, S., 2005. Assessing the completeness of optical resetting of quartz OSL in the natural environment. Radiation Measurements 40, 13-25.

Smith, B.W., Aitken, M.J., Rhodes, E.J., Robinson, P.D., Geldard, D.M., 1986. Optical dating: methodological aspects. Radiation Protection Dosimetry 17, 229-233.

Smith, B.W., Rhodes, E.J., 1994. Charge movements in quartz and their relevance to optical dating. Radiation Measurements 23, 329-333.

Sohbati, R., Murray, A.S., Buylaert, J.-P., Almeida, N.A.C., Cunha, P.P., 2012. Optically stimulated luminescence (OSL) dating of quartzite cobbles from the Tapada do Montinho archaeological site (east-central Portugal). Boreas 41, 452-462.

Spooner, N.A., 1994. On the optical dating signal from quartz. Radiation Measurements 23, 593-600.

Spooner, N.A., Franklin, A.D., 2002. Effect of the heating rate on the red TL of quartz. Radiation Measurements 35, 59-66.

Spooner, N.A., Questiaux, D.G., 2000. Kinetics of red, blue and UV thermoluminescence and optically-stimulated luminescence from quartz. Radiation Measurements 32, 659-666.

Subedi, B., Kitis, G., Pagonis, V., 2010. Simulation of the influence of thermal quenching on thermoluminescence glow-peaks. Phys. Status Solidi A 207, 1216-1226.

Subedi, B., Oniya, E., Polymeris, G.S., Afouxenidis, D., Tsirliganis, N.C., Kitis, G., 2011. Thermal quenching of thermoluminescence in quartz samples of various origin. Nuclear Instruments and Methods in Physics Research B, 269, 572-581.

Subedi, B., Polymeris, G.S., Tsirliganis, N.C., Pagonis, V., Kitis, G., 2012. Reconstruction of thermally quenched glow curves in quartz. Radiation Measurements 47, 250-257.

Thiel, C., Buylaert, J.-P., Murray, A.S., Elmejdoub, N., Jedoui, Y., 2012. A comparison of TT-OSL and post-IR IRSL dating of coastal deposits on Cap Bon peninsula, north-eastern Tunisia. Quaternary Geochronology 10, 209-217.

Timar, A., Vanderberghe, D., Panaiotu, C.E., Panaiotu, C.G., Necula, C., Cosma. C., Van den Haute, P., 2010. Optical dating of Romanian loess using fine-grained quartz. Quaternary Geochronology 5, 143-148.

Timar-Gabor, A., Vandenberghe, D.A.G., Vasiliniuc, Ş., Panaoitu, C.E., Panaiotu, C.G., Dimofte, D., Cosma, C., 2011. Optical dating of Romanian loess: A comparison between silt-sized and sand-sized quartz. Quaternary International 240, 62-70.

Timar-Gabor, A., Vasiliniuc, Ş., Vandenberghe, D.A.G., Cosma, C., Wintle, A.G., 2012. Investigations on the reliability of SAR-OSL equivalent doses obtained for quartz samples displaying dose response curves with more than one component. Radiation Measurements 47, 740-45.

Timar-Gabor, A., Buylaert, J-P., Guralnik, B., Trandafir-Antohi, O., Constantin, D., Anechtei, V., Jain, M., Murray, A.S., Porat, N., Hao, Q., Wintle, A.G., 2017. On the importance of grain size in luminescence dating using quartz. Radiation Measurements. 10.1016/j.radmeas.2017.01.009

Timar-Gabor, A., Wintle, A.G., 2013. On natural and laboratory generated dose response curves for quartz of different grain sizes from Romanian loess. Quaternary Geochronology, 18, 34-40.

Toyoda, S., 2015. Paramagnetic lattice defects in quartz for applications to ESR dating. Quaternary Geochronology 30, 498-505.

Toyoda, S., Nagashima, K., Yamamoto, Y., 2016. ESR signals in quartz: Applications to provenance research – A review. Quaternary International 397, 258–266.

Trandafir, O., Timar-Gabor, A., Schmidt, C., Veres, D., Anghelinu, M., Hambach, U., Simon, S., 2015. OSL dating of fine and coarse quartz from a Palaeolithic sequence on the Bistrita Valley (Northeastern Romania). Quaternary Geochronology 30, 487-492.

Tsukamoto, S., Murray, A., Ankjærgaard, C., Jain, M., Lapp, T., 2010. Charge recombination processes in minerals studied using optically stimulated luminescence and time-resolved exo-electrons. Journal of Physics D 43, 325502 (9 pp).

Vandenberghe, D.A.G., Jain, M., Murray, A.S., 2009. Equivalent dose determination using a quartz isothermal TL signal. Radiation Measurements 44, 439-444.

Wallinga, J., Bos, A.J.J., Duller, G.A.T., 2008. On the separation of quartz OSL signal components using different stimulation modes. Radiation Measurements 43, 742-747.

Wallinga, J., Hobo, N., Cunningham, A.C., Versendaal, A.J., Makaske, B., Middelkoop, H., 2010. Sedimentation rates on embanked floodplains determined through quartz optical dating. Quaternary Geochronology 5, 170-175.

Wang, X.L., Wintle, A.G., Lu, Y.C., 2006a. Thermally transferred luminescence in fine-grained quartz from Chinese loess: Basic Observations. Radiation Measurements 41, 649-658.

Wang, X.L., Lu, Y.C., Wintle, A.G., 2006b. Recuperated OSL dating of fine-grained quartz in Chinese loess. Quaternary Geochronology 1, 89-100.

Wang, X.L., Wintle, A.G., Adamiec, G., 2012. Improving the reliability of single-aliquot regenerative dose dating using a new method of data analysis. Quaternary Geochronology 9, 65-74.

Wang, X.L., Wintle, A.G., Lu, Y.C., 2007. Testing a single-aliquot protocol for recuperated OSL dating. Radiation Measurements 42, 380-391. Wang, X.L., Du, J.H., Adamiec, G., Wintle, A.G., 2015. The origin of the medium OSL component in West Australian quartz. Journal of Luminescence 159, 147-157.

Watanuki, T., Murray, A.S., Tsukamoto, S., 2003. A comparison of OSL ages derived from silt-sized quartz and polymineral grains from Chinese loess. Quaternary Science Reviews 22, 991-997.

Watanuki, T., Murray, A.S., Tsukamoto, S. (2005) Quartz and polymineral luminescence dating of Japanese loess over the last 0.6 Ma: Comparison with an independent chronology. Earth and Planetary Science Letters 240, 774-789.

Wintle, A.G., 1975. Thermal quenching of thermoluminescence in quartz. Geophysical Journal of the Royal Astronomical Society 41, 107-113.

Wintle, A.G., 2010. Future directions of luminescence dating of quartz. Geochronometria 37, 1-7.

Wintle, A.G., Murray, A.S., 1997. The relationship between quartz thermoluminescence, photo-transferred thermoluminescence and optically stimulated luminescence. Radiation Measurements 27, 611-624.

Wintle, A.G., Murray, A.S., 2006. A review of quartz optically stimulated luminescence characteristics and their relevance in single-aliquot regeneration dating protocols. Radiation Measurements 41, 369-391.

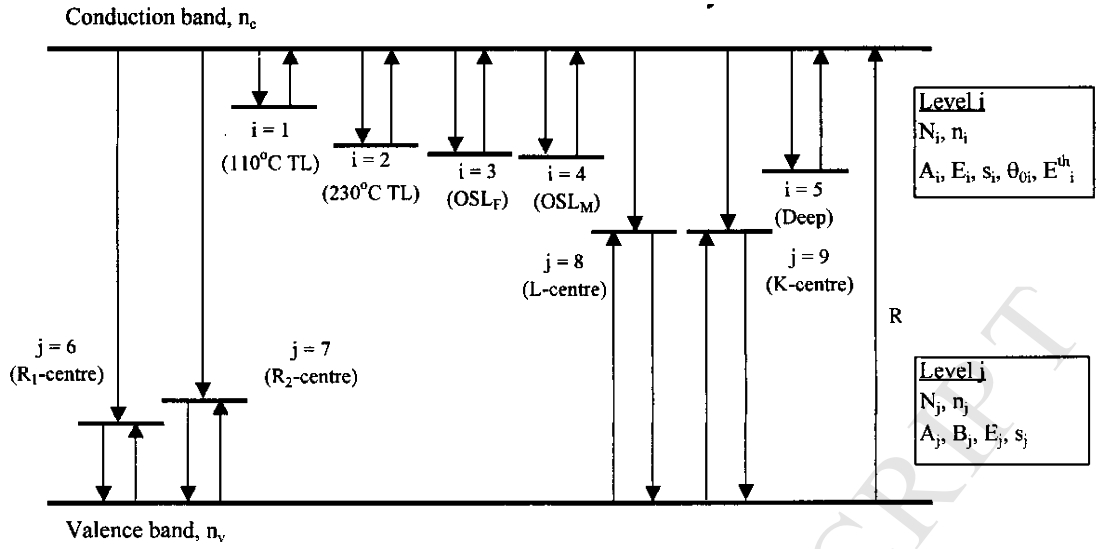

Figure 1 (redrawn from Bailey, 2001) Energy level diagram showing different traps and recombination centres and allowable transitions.

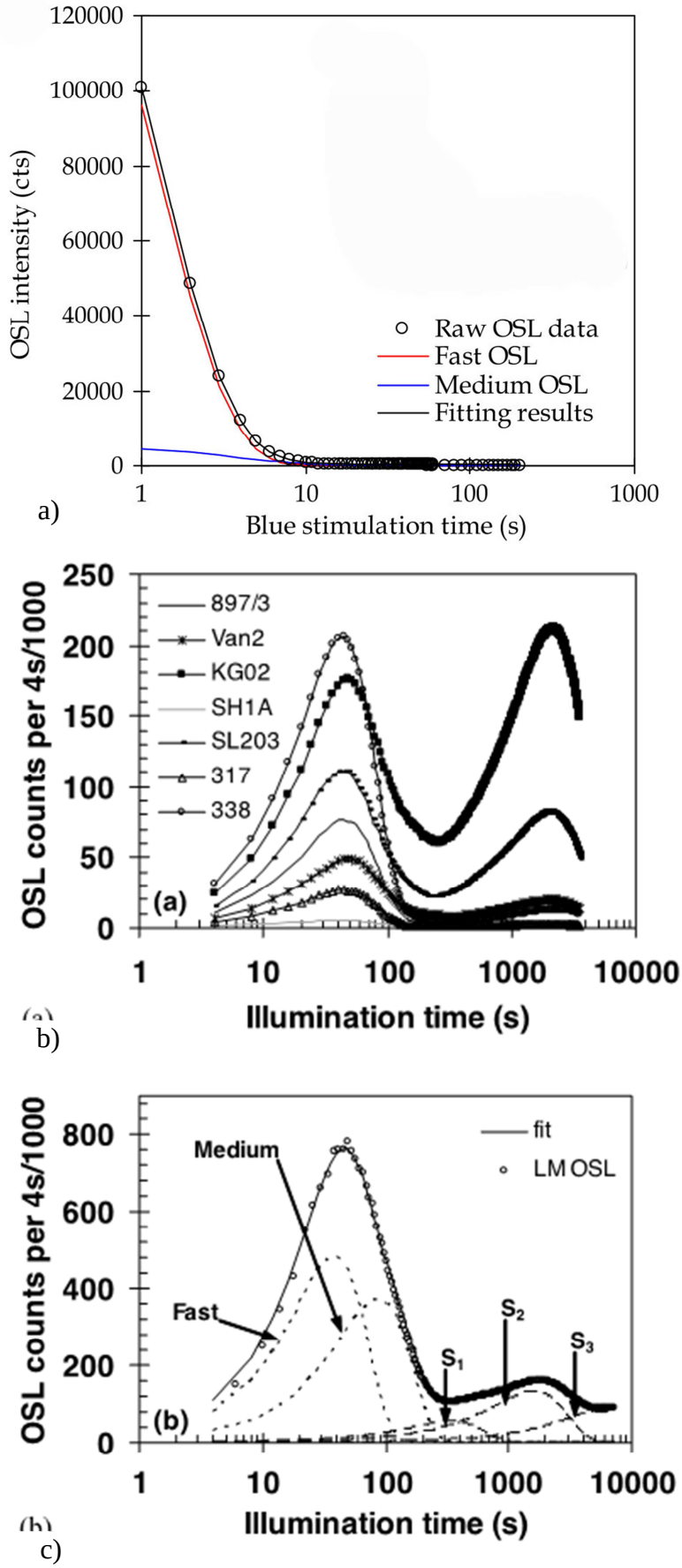

Figure 2 a) an example of a CW-OSL decay curve with a fitted fast and medium component shown (from Wang et al. 2012) b) LM-OSL curves of seven samples and c) deconvolution of the LM-OSL curve from sample SL203 (from b) into 5 first order components (both b and c from Singarayer and Bailey, 2003).

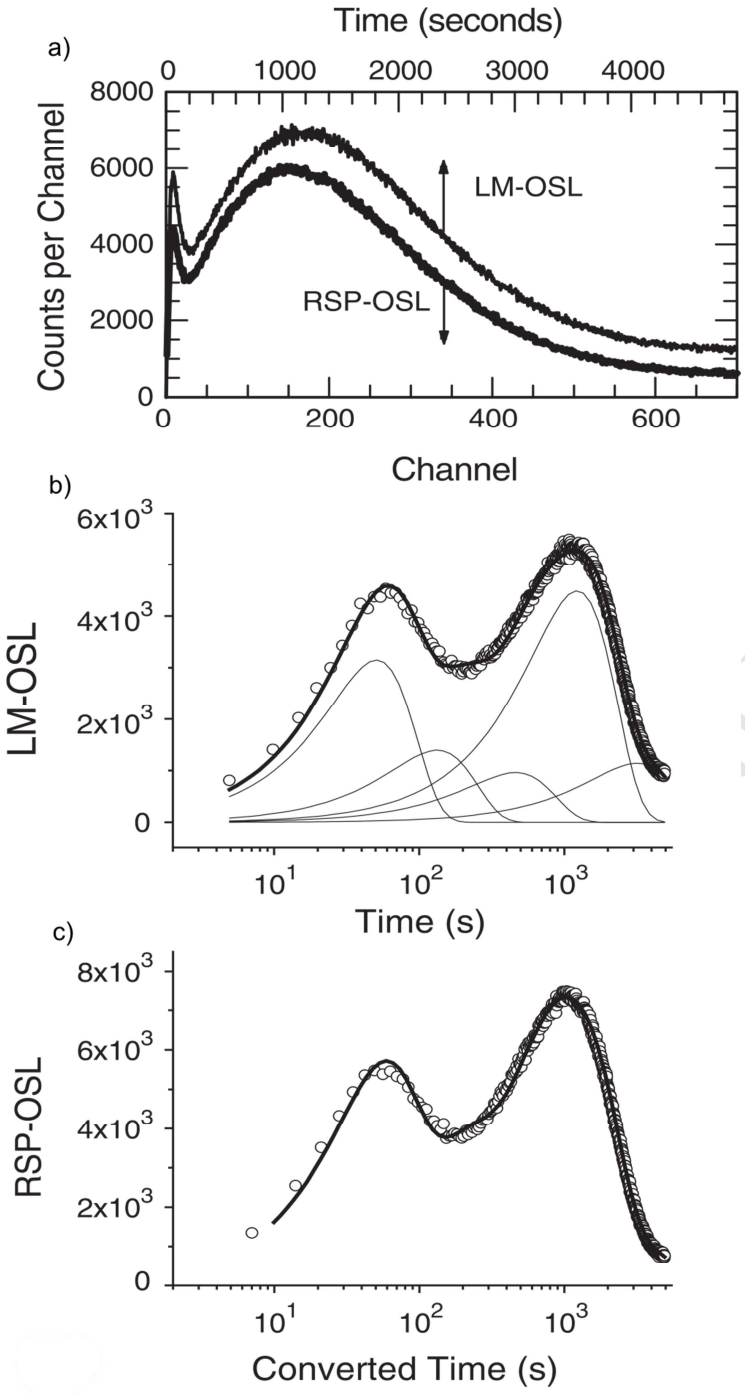

Figure 3 (from Poolton et al., 2003) comparing LM-OSL with RSP-OSL of a quartz sample, a) as the data are collected, b) LM-OSL as a function of stimulation time and c) RSP-OSL after a mathematical transformation enables the data to be plotted as a function of time.

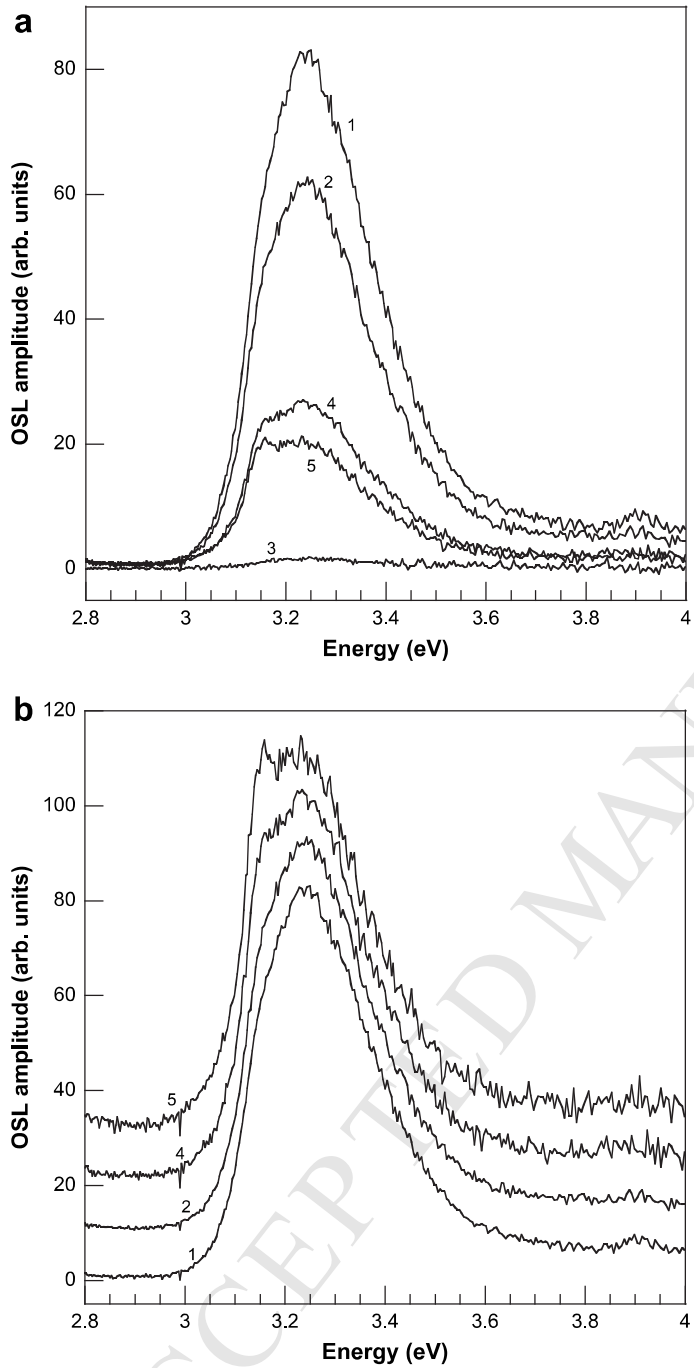

Figure 4 (from Martini et al., 2009) OSL spectra for a synthetic quartz obtained under optical stimulation in time intervals (1) 5-45 s, (2) 45-85 s, (3) 85-125 s, without stimulation, (4) 125-165 s, and (5) 165-205 s). (a) The data as collected, and (b) after normalisation (and offset) for (1), (2), (4) and (5). The energy scale shown corresponds to 443 to 310 nm.

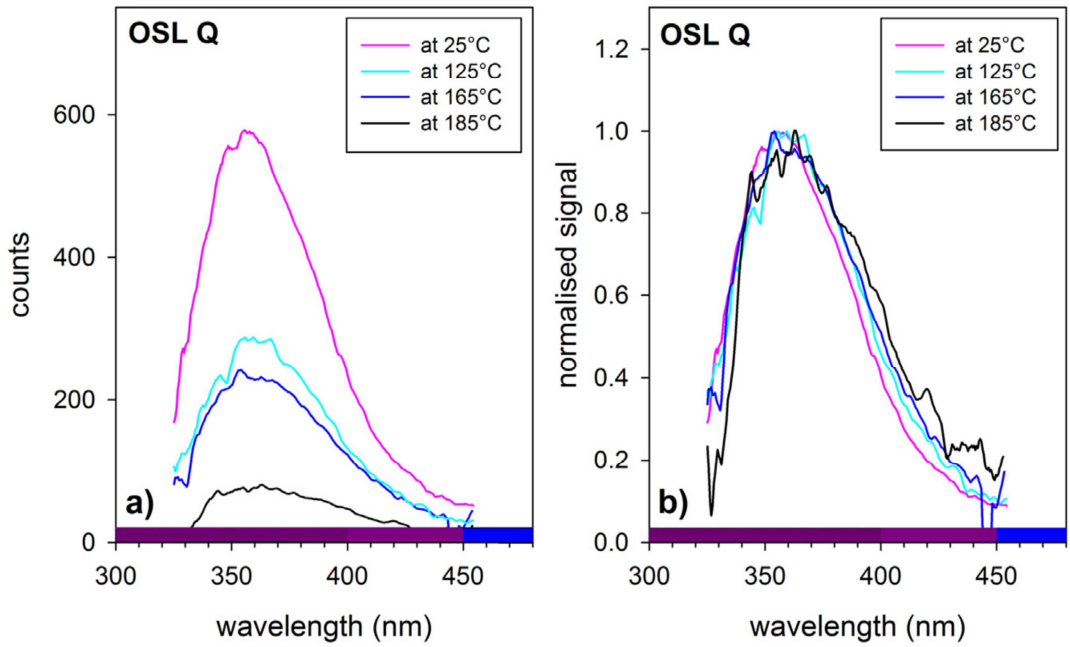

Figure 5 (from Lomax et al., 2015) OSL spectra for natural quartz obtained during optical stimulation with 525 nm photons at four different temperatures (a) corrected for efficiency of detector and (b) data from (a) normalised to maximum of 1. The wavelength scale shown corresponds to 4.13 eV to 2.58 eV.

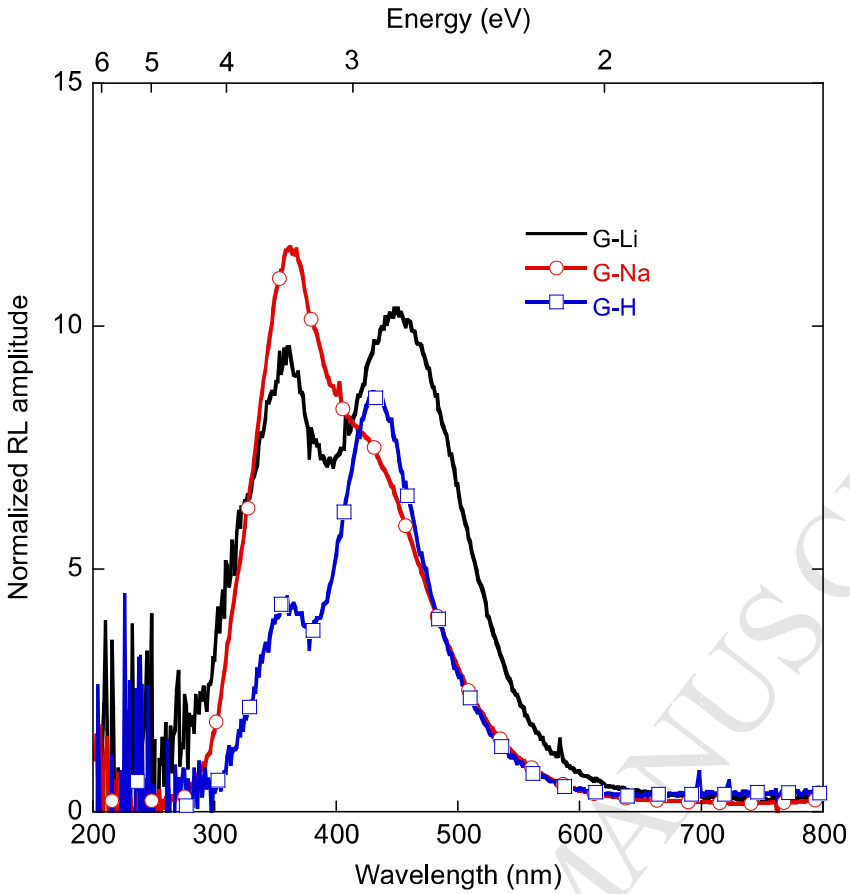

Figure 6 (from Martini et al., 2012a) RL spectra obtained during irradiation with X-rays for synthetic quartz samples in which H^+, Na^+ and Li^+ ions had been swept in.

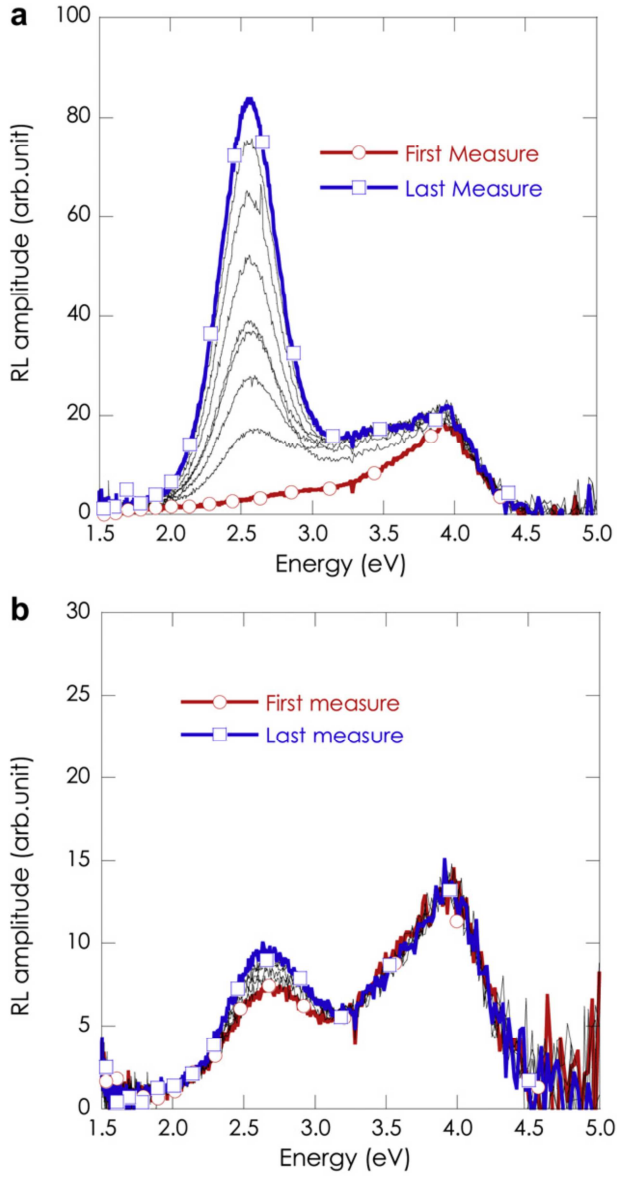

Figure 7 (from Martini et al., 2012b) Repeated RL spectra obtained under X-rays with a dose of 10 Gy being given in each run (a) natural quartz, (b) synthetic quartz. The energy scale shown corresponds to 827 nm to 248 nm.

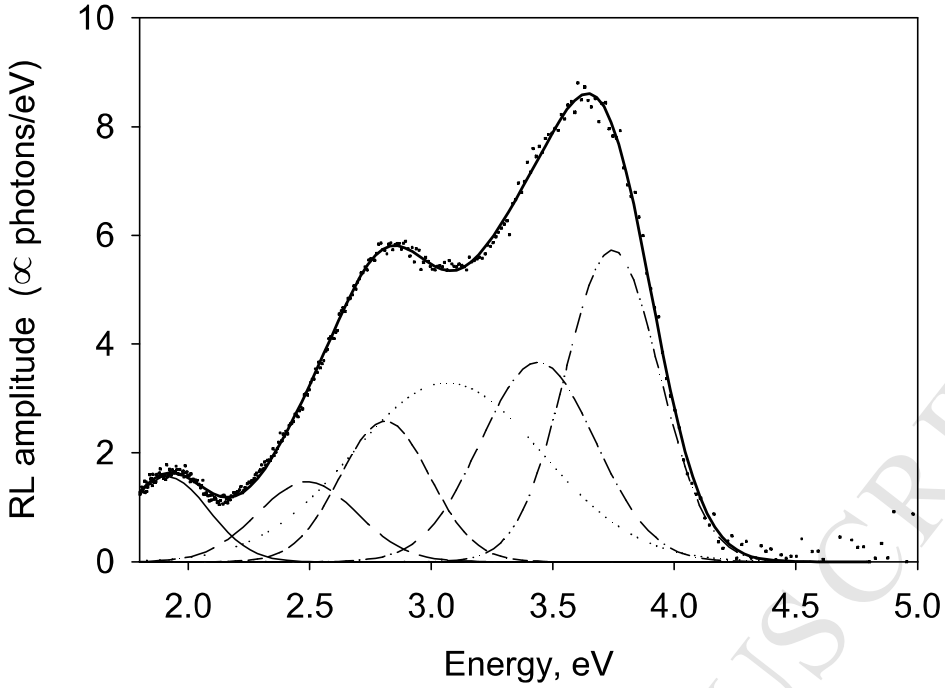

Figure 8 (from Pagonis et al., 2014) Deconvolution of RL spectra into 7 Gaussian components for a sample of commercially-available natural quartz previously heated to 700°C. The energy scale shown corresponds to 708 nm to 248 nm.

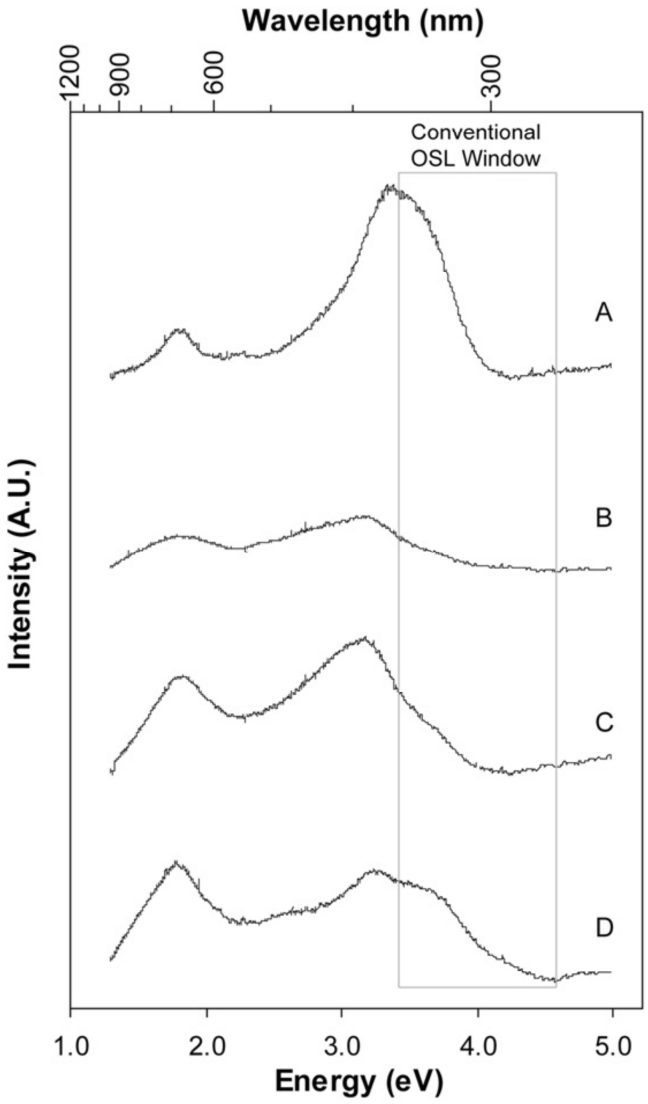

Figure 9 (from King et al., 2011) Ionoluminescence spectra from four natural quartz samples (A, B, C, D) measured at room temperature for 190 s when stimulated with 0.95 MeV protons. A is calibration quartz.

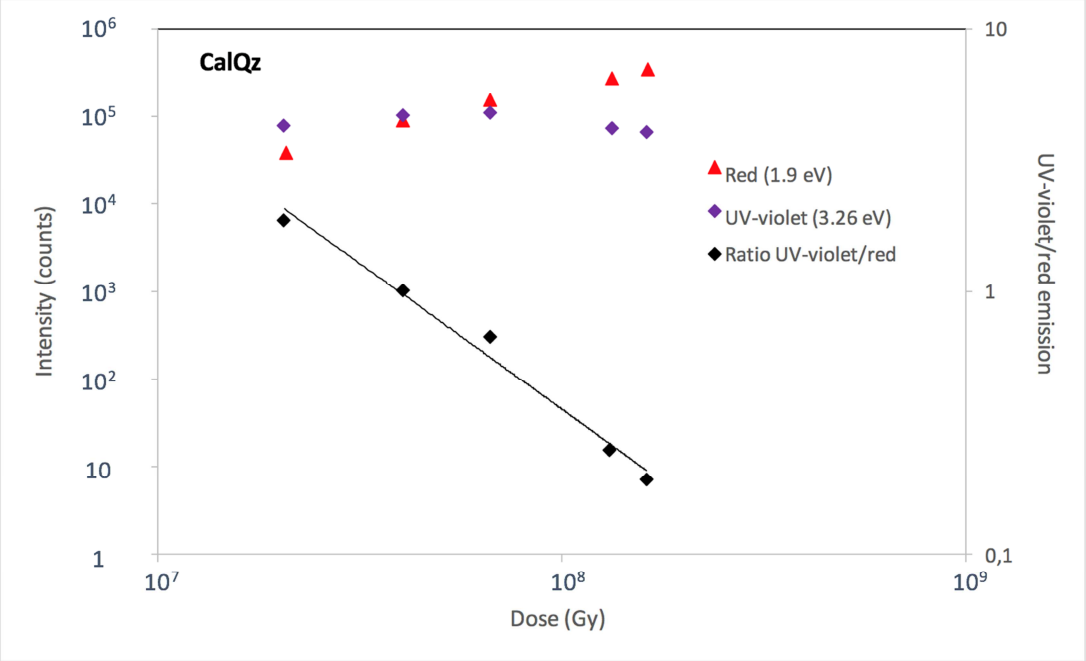

Figure 10 (modified from King et al., 2011) Red and UV/violet ionoluminescence signals (and their ratio) as a function of dose delivered as measured for calibration quartz by repeated runs in which doses of ~$4x10^7$ Gy are delivered.

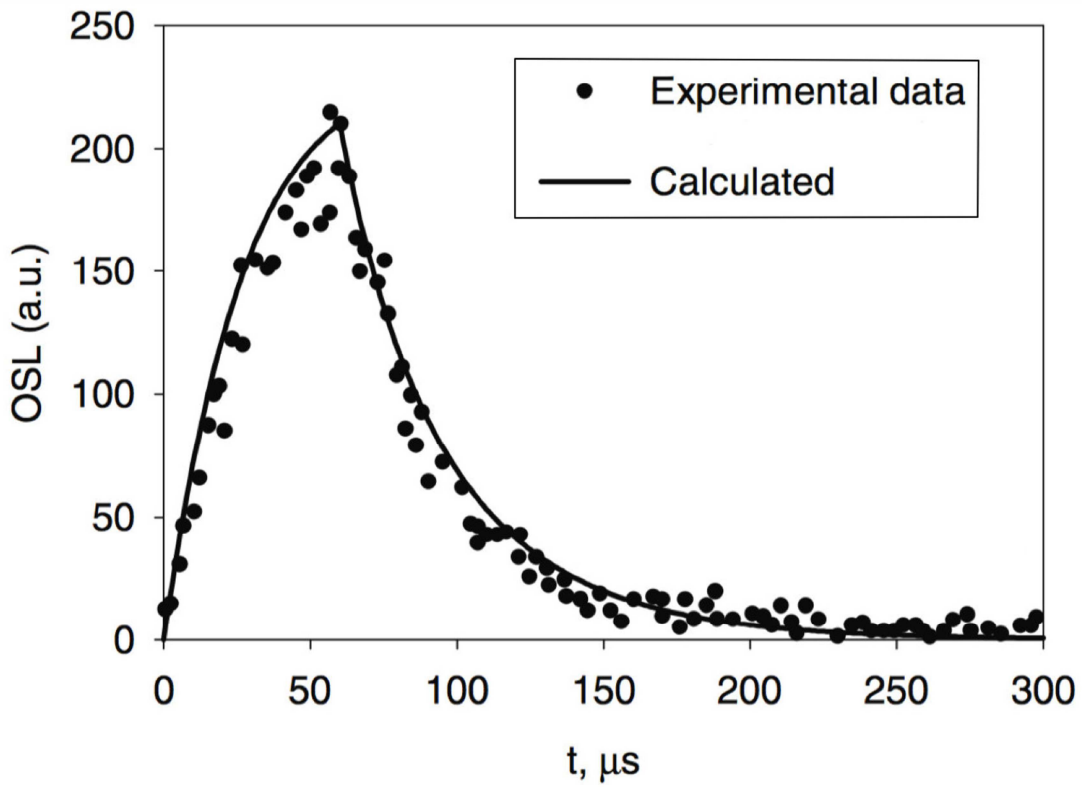

Figure 11 (from Pagonis et al., 2009b) Comparison of experimental data with results of simulations for time-resolved luminescence.

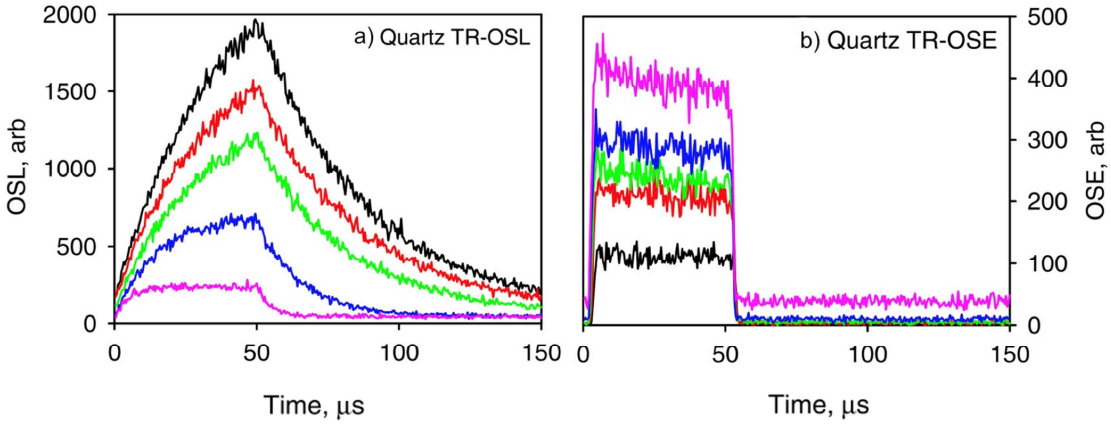

Figure 12 (from Tsukamoto et al., 2010) Time-resolved (TR) OSL (a) and OSE (b) from quartz measured at stimulation temperatures of 50, 100, 150, 200 and 250°C using pulsed LED stimulation with on-time of 50 µs and off-time of 100 µs.

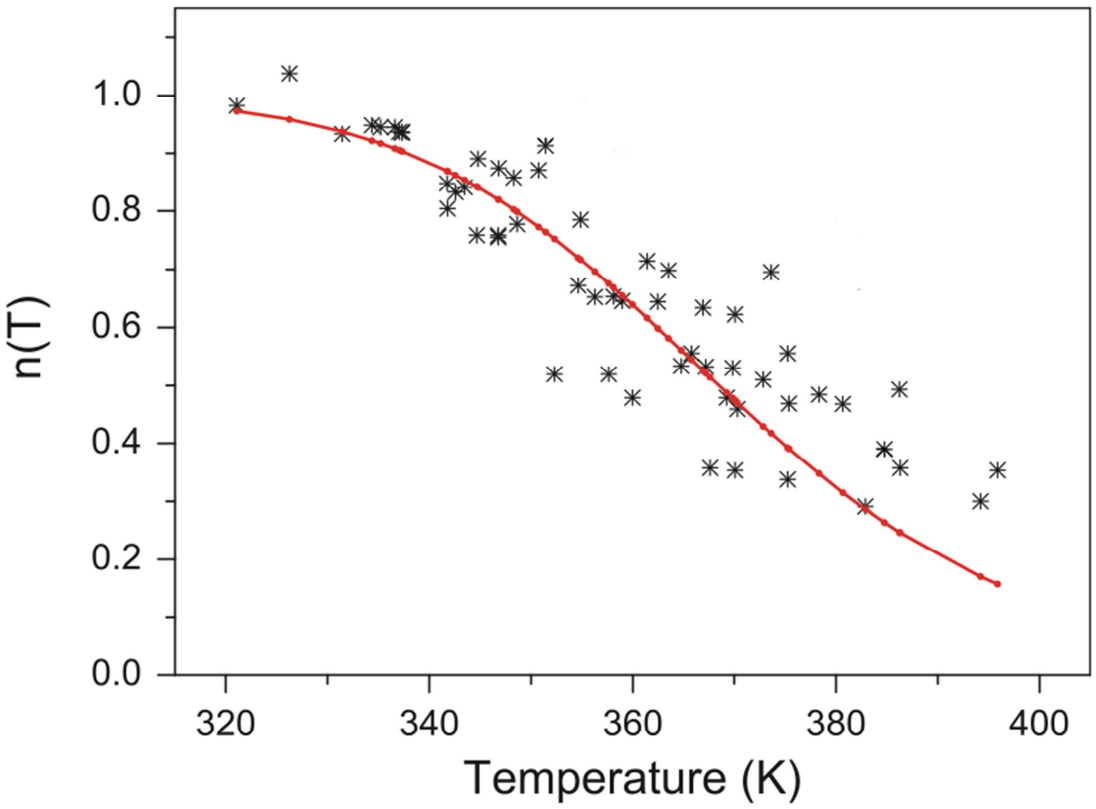

Figure 13 (modified from Subedi et al., 2011) Luminescence efficiency as a function of temperature obtained by measurement of the "110°C" peak for different heating rates, and calculated using the parameters of Petrov and Bailiff (1997).

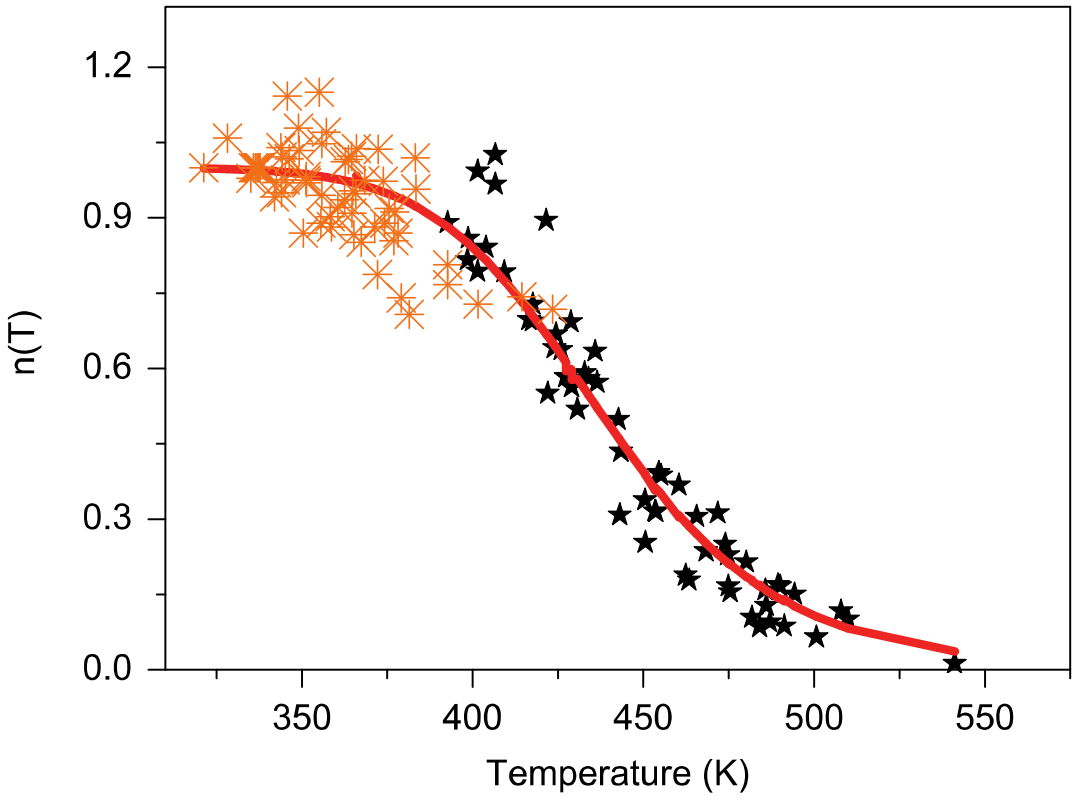

Figure 14 (from Subedi et al., 2011) Luminescence efficiency measured as for Fig. 13, but over an extended temperature region using two additional peaks. Crosses are for the 110°C peak and stars for the higher temperature peaks, and the line represents values calculated using the parameters of Wintle (1975).

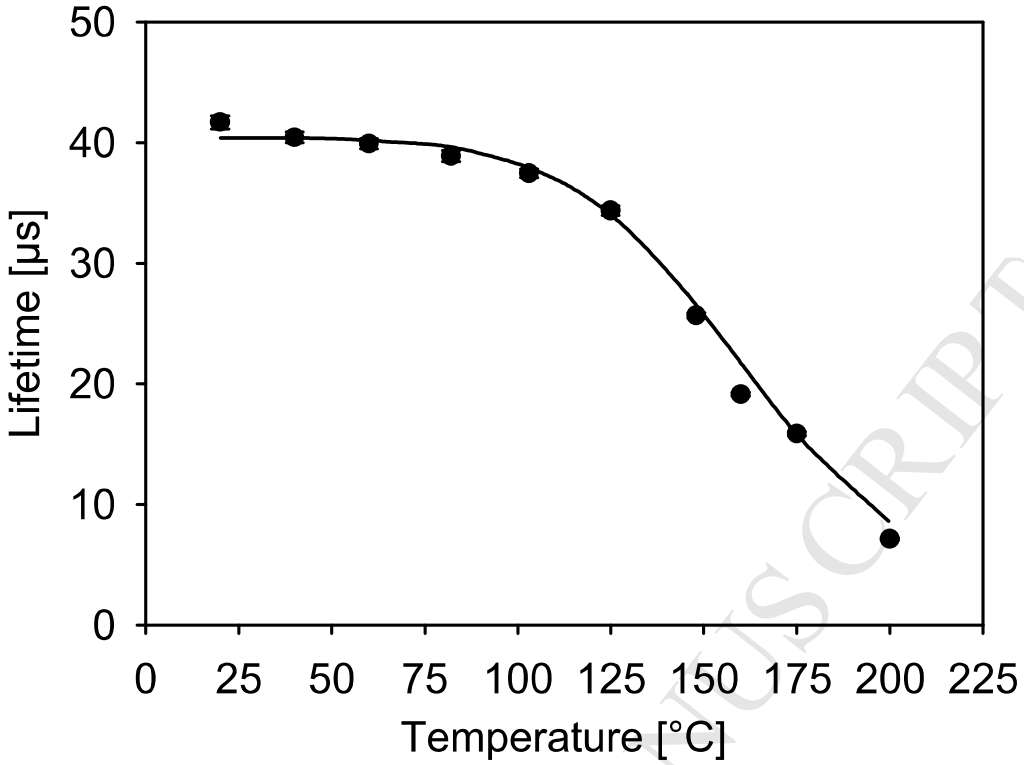

Figure 15 (from Chithambo, 2003) The lifetime of the time-resolved OSL measured using pulsed stimulation at 525 nm as a function of the stimulation temperature.

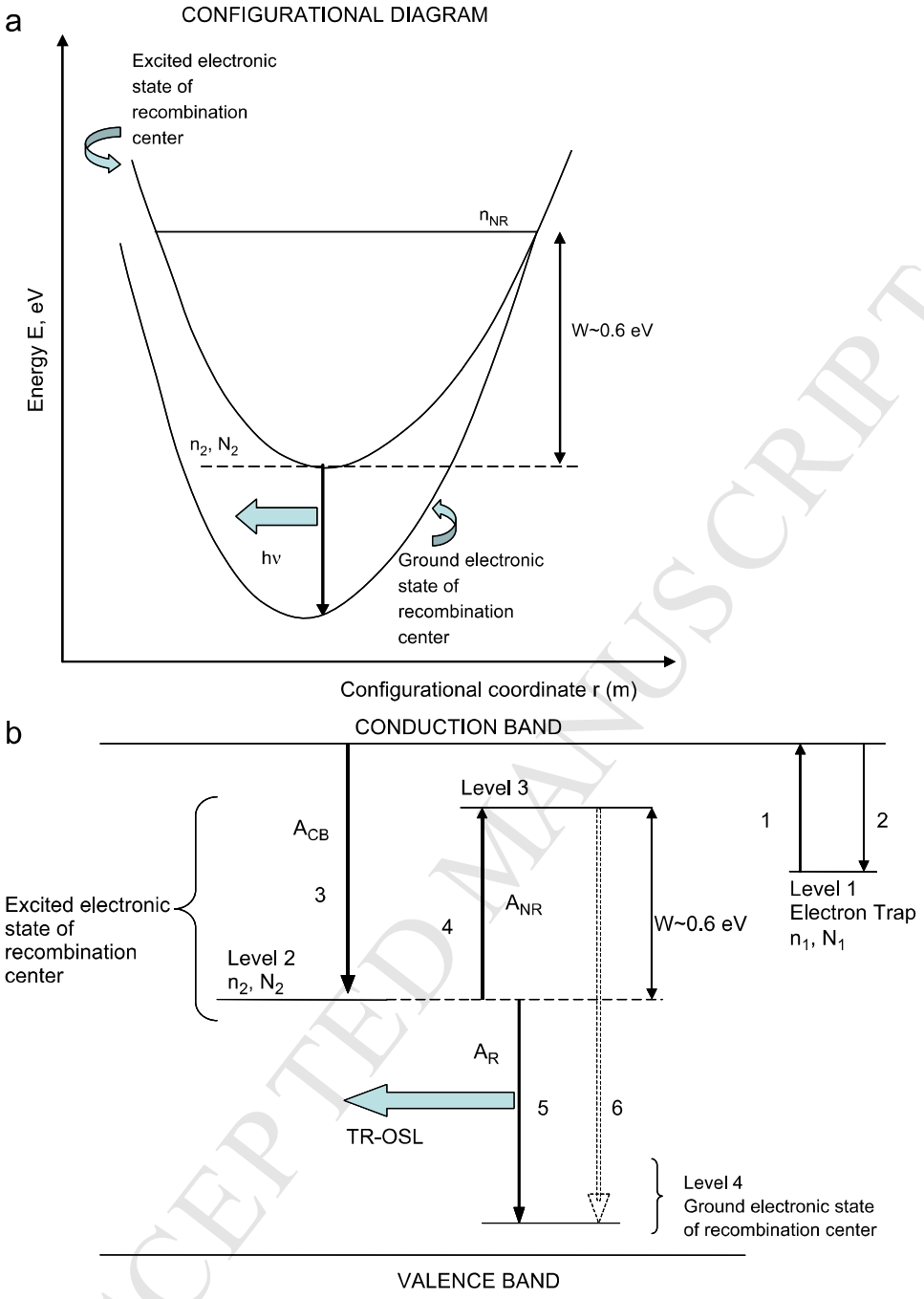

Figure 16 (from Pagonis et al., 2010) (a) Configurational coordinate diagram outlining the Mott-Seitz mechanism in quartz. (b) Energy level diagram based on the Mott-Seitz model and related to production of TR-OSL

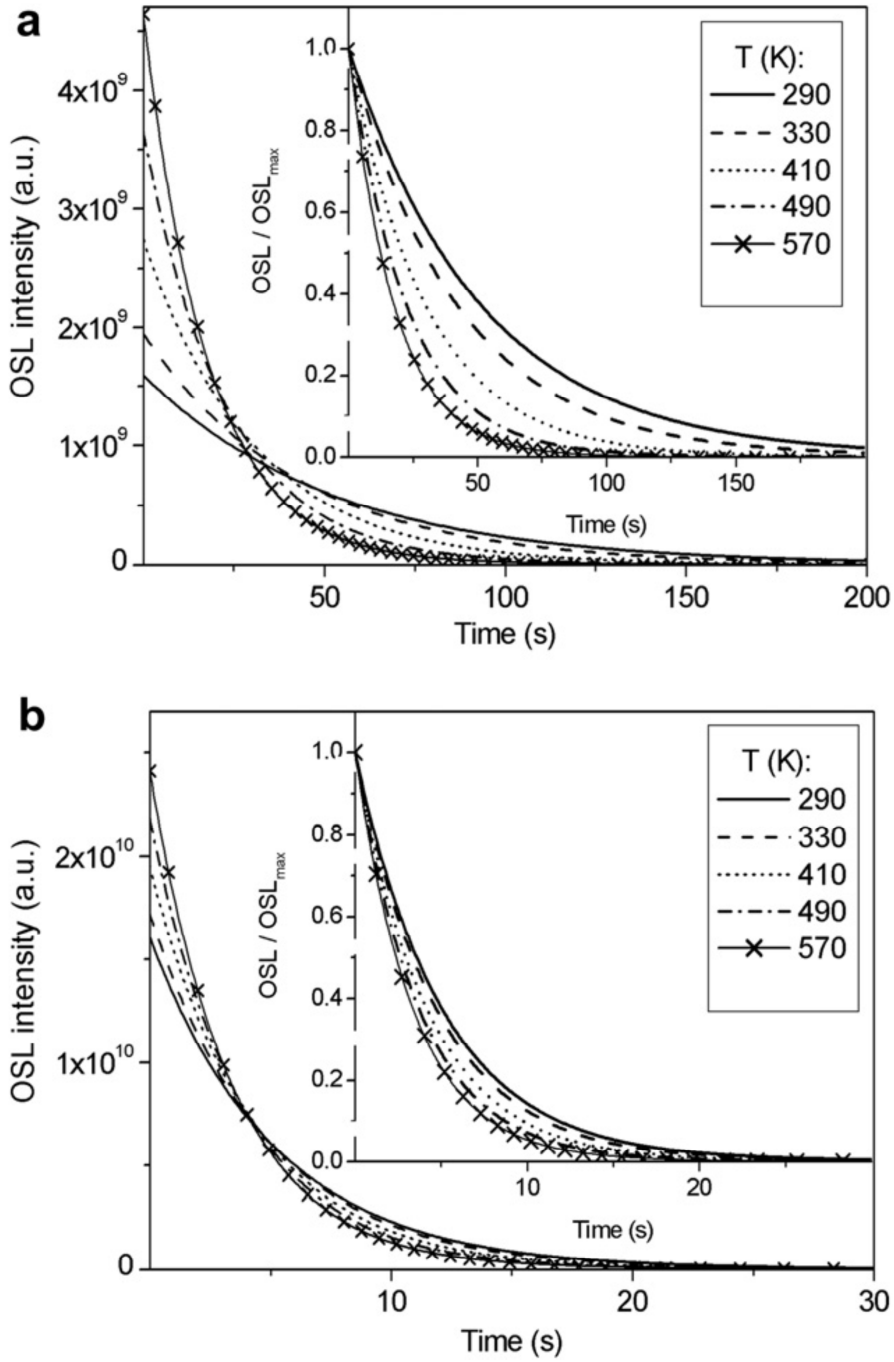

Figure 17 (from Chruścińska, 2010) OSL decay curves obtained at temperatures ranging from 290 to 570 K calculated using a model with a single optical trap (E_0 = 2.0 eV) and using stimulating wavelengths (hν) of (a) 1.9 eV and (b) 2.0 eV). Inset shows data normalised to initial value.

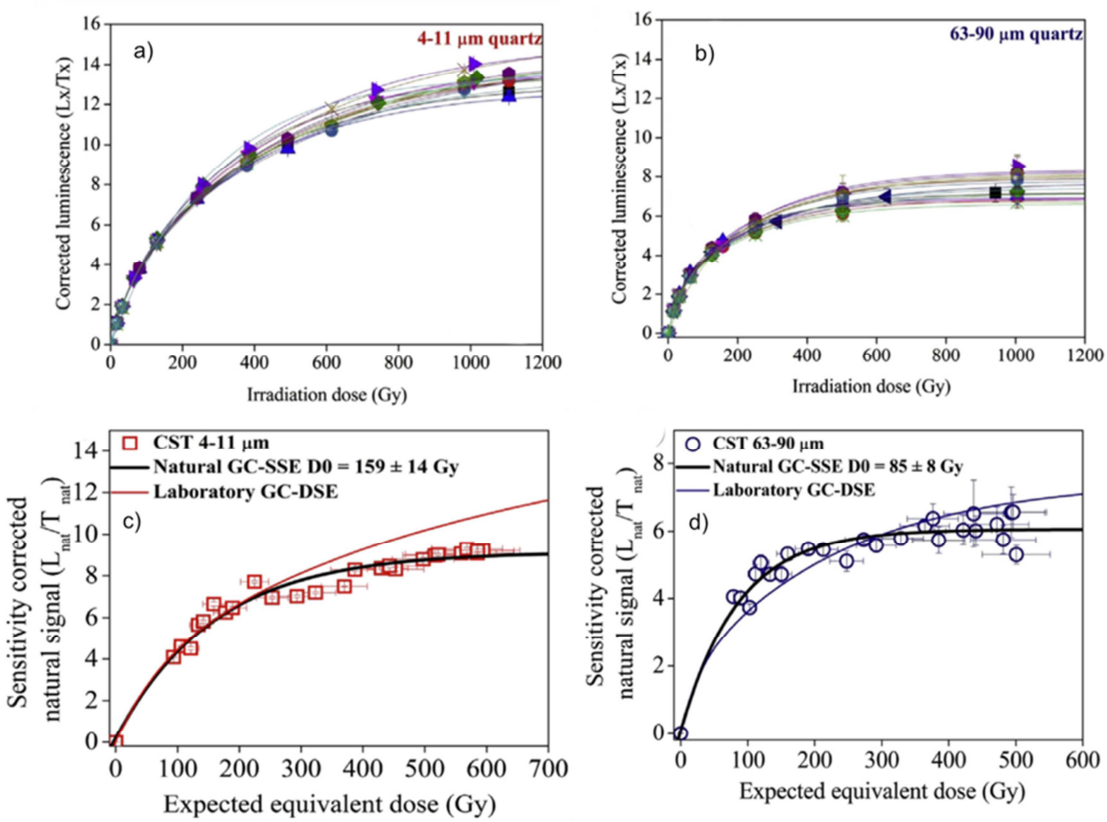

Figure 18 (modified from Timar-Gabor and Wintle, 2013) Laboratory dose response curves obtained using a SAR protocol for samples of loess from Costineşti, Romania (a) for 4-11 µm grains and (b) 63-90 µm grains. (c) and (d) averaged dose response curves using data from (a) and (b) fitted with double exponential function (GC-DSE) and average values for sensitivity-corrected natural values for the same samples fitted with a single exponential function (GC-SSE).

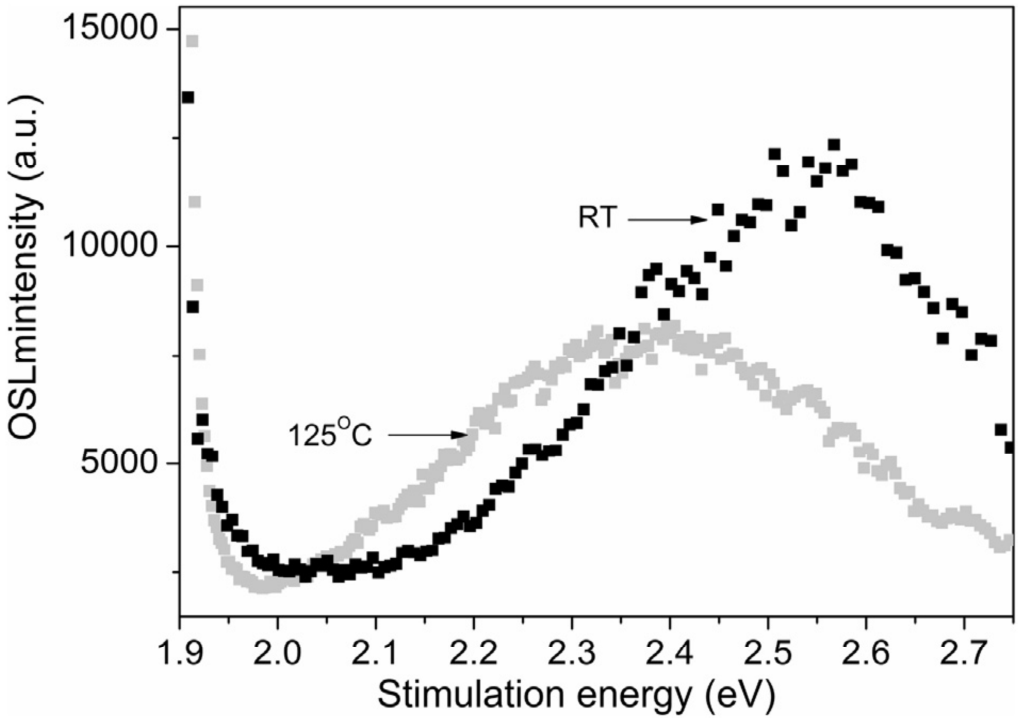

Figure 19 (from Chruścińska, 2014) Examples of experimentally obtained curves in VES-OSL measurements at room temperature and 125°C. The scans were obtained after irradiation with 70 Gy using a scanning rate of 0.0012 eV s^{-1}. The energy scale shown corresponds to 653 nm to 451 nm.

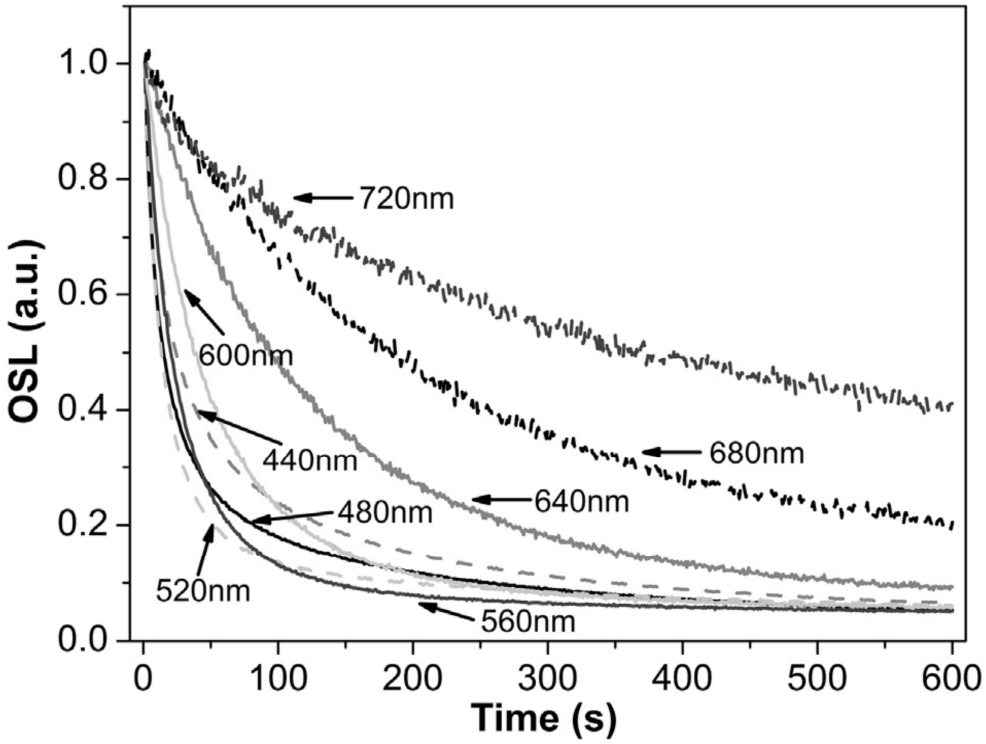

Figure 20 (from Kijek et al., 2014) OSL decay curves taken at room temperature normalised to the initial value when stimulation was carried out using the indicated wavelengths of stimulating light. The quartz grains extracted from a brick were irradiated in the laboratory with a dose of about 690 Gy and stored for at least a day.

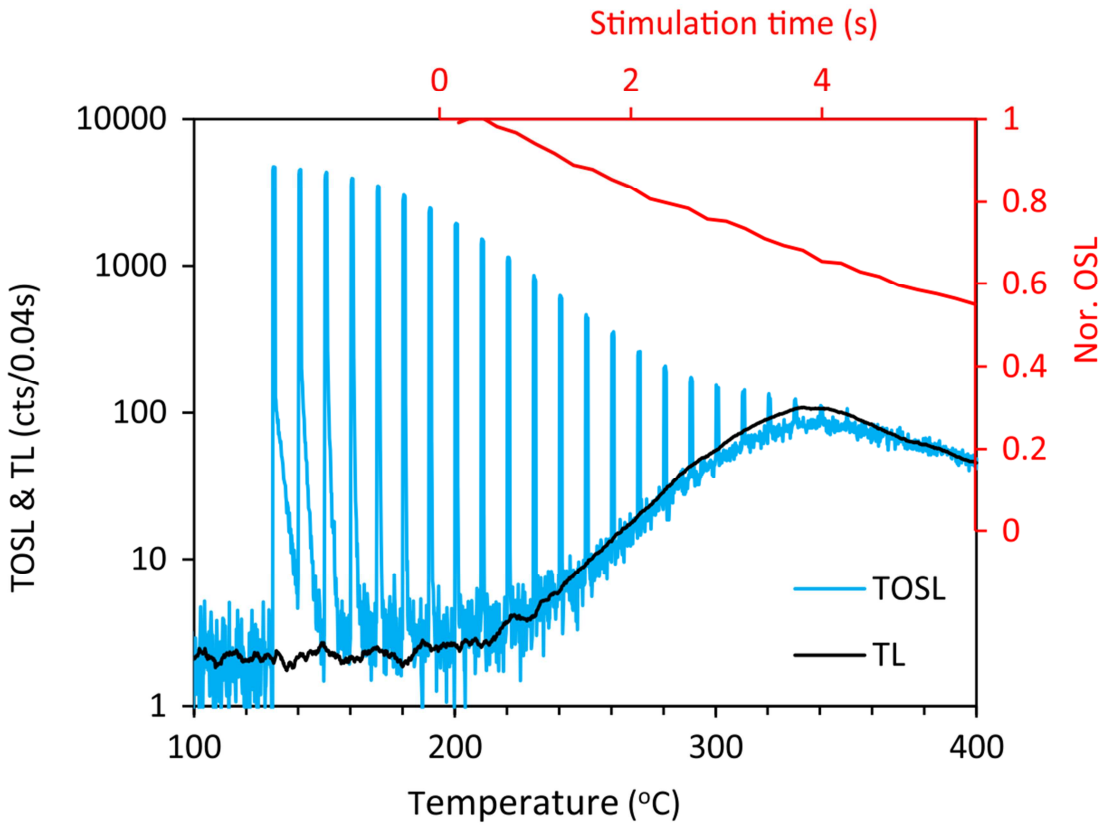

Figure 21 (from Wang et al., 2015) (a) TOSL curve obtained as TL glow curve with pulsed optical stimulation and TL glow curve obtained without optical stimulation, both after preheating at 260°C for 10 s; top right shows CW-OSL stimulated at 125°C with power of 1.92 mW/s for 5.8 s.

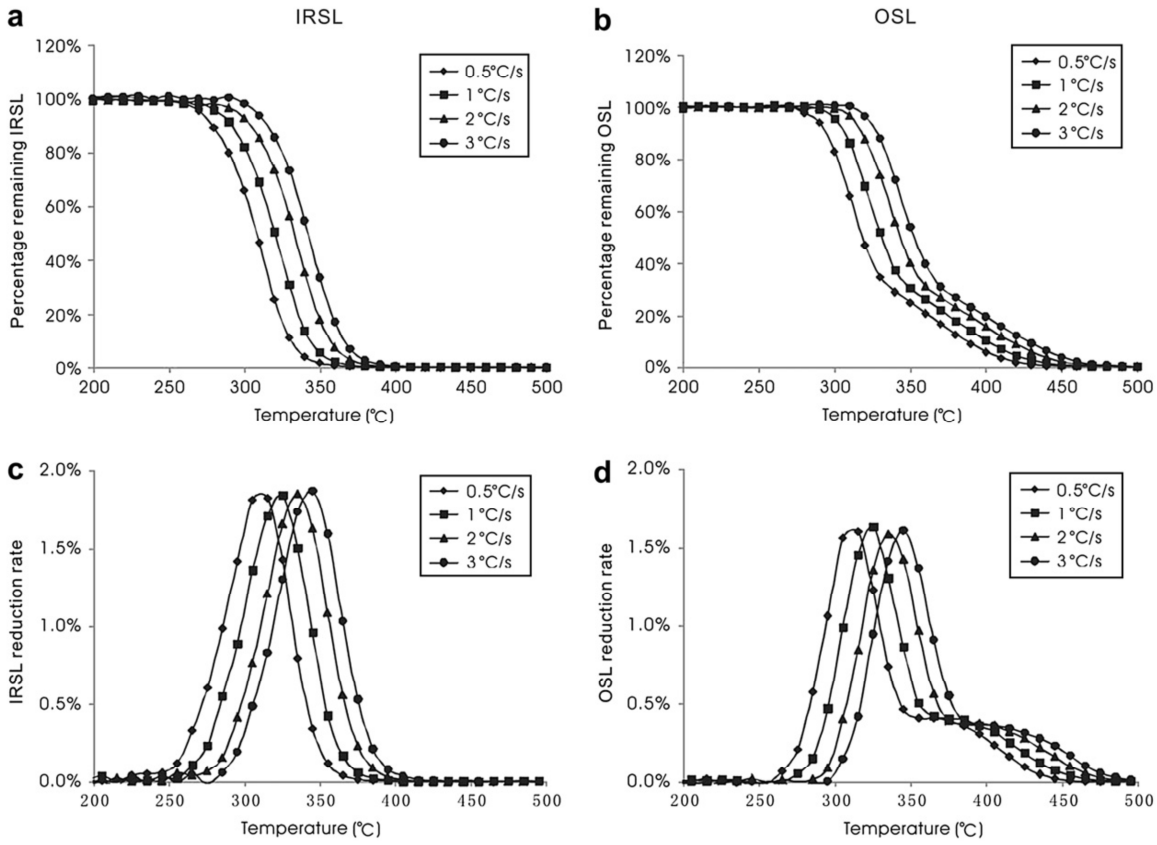

Figure 22 (from Fan et al., 2009) a) and b) show pulse annealing curves of the 40 s IRSL and 0.1 s OSL signals. The IRSL was recorded at 150°C. The plots c) and d) show reduction of the respective signal per °C.

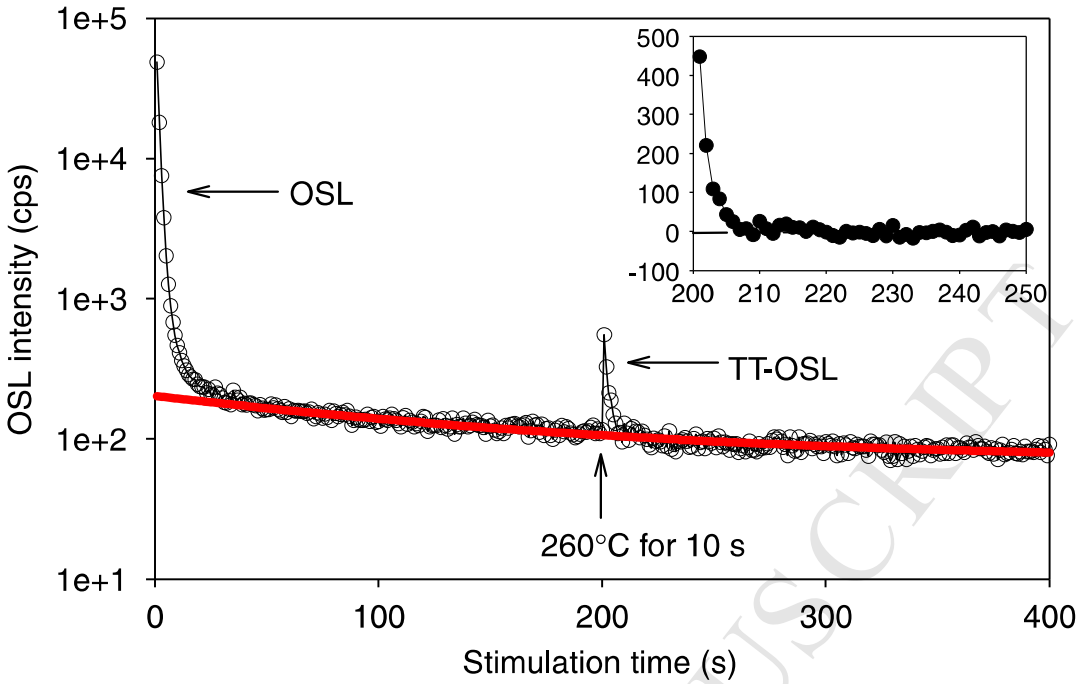

Figure 23 (from Wang et al., 2006a) OSL signal measured at 125°C as a function of stimulation time, following a natural radiation dose of ~200 Gy. After 200 s of optical stimulation, the aliquot is heated at 260°C for 10 s and the optical stimulation at 125°C recommences and results in the TT-OSL signal. The inset shows the TT-OSL signal on a linear scale, following subtraction of the background signal from slow OSL components.

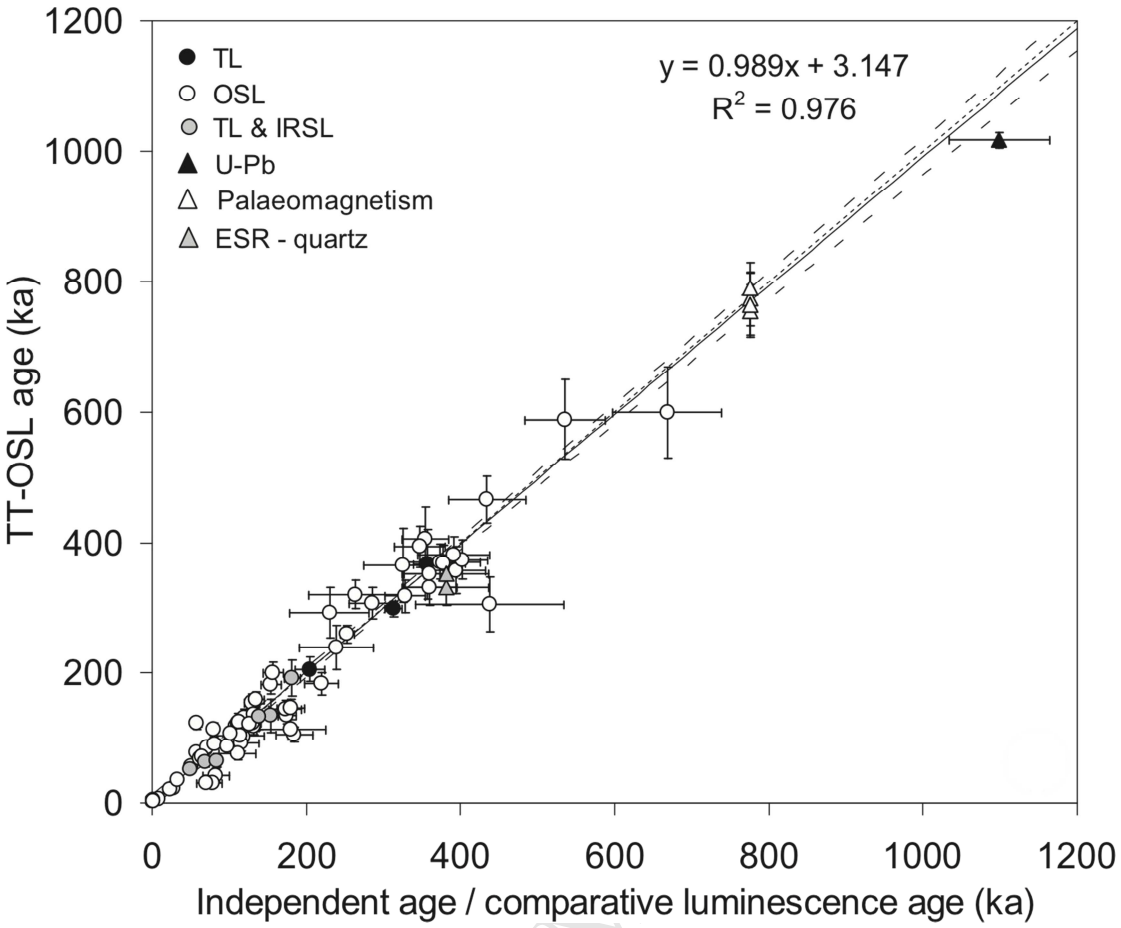

Figure 24 (from Arnold et al., 2015) TT-OSL ages versus independent age estimates or semi-independent age estimates obtained using conventional luminescence dating methods (TL, fading-corrected IRSL, OSL).

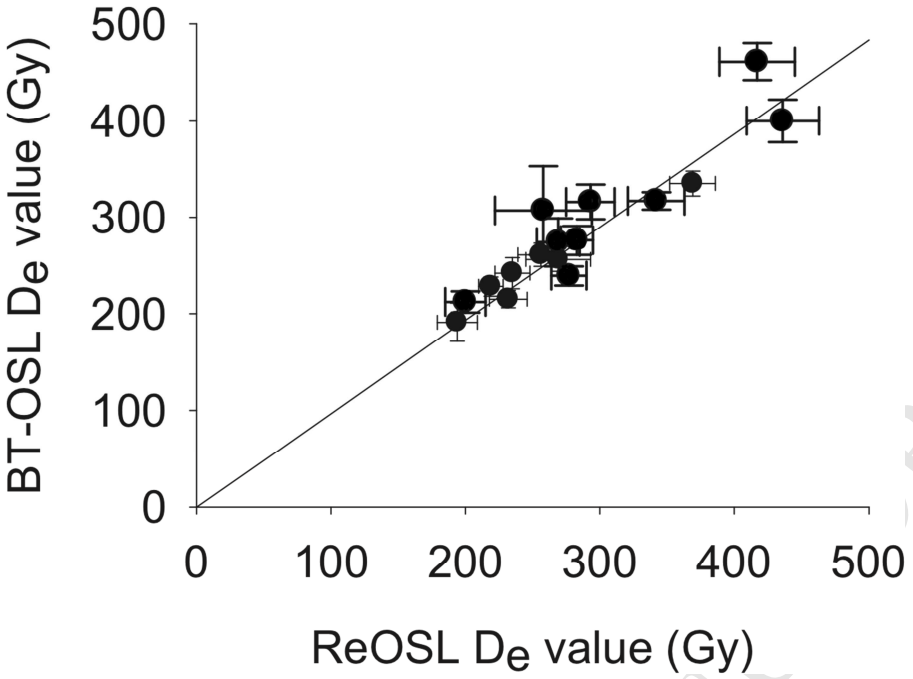

Figure 25 (from Jacobs et al., 2011) BT-OSL D_e values plotted as a function of their ReOSL D_e values for Middle Pleistocene sands from the southern South African coast.

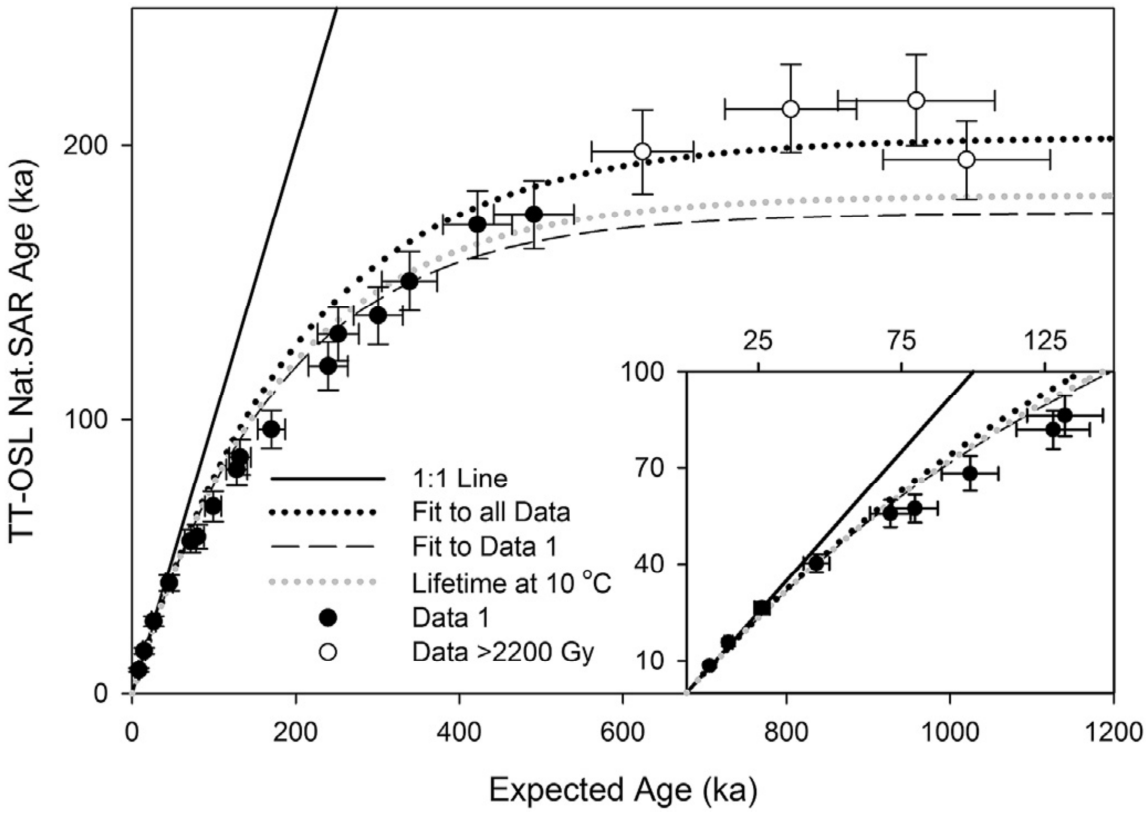

Figure 26 (from Chapot et al., 2016) TT-OSL ages obtained with a SAR protocol plotted against independently determined ages for the loess section at Luochuan. The results deviate from the 1:1 line for samples as young as 45 ka.

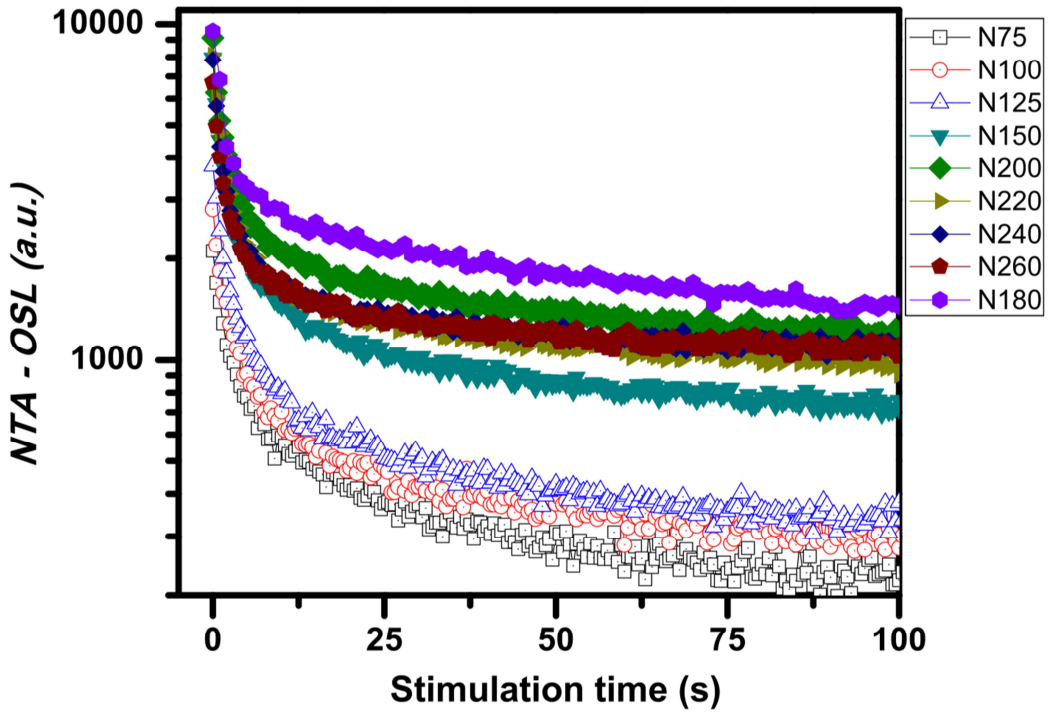

Figure 27 (from Polymeris et al., 2015) Natural TA-OSL curves recorded at temperatures ranging from 75°C up to 260°C.

Highlights

1) Review of OSL signals in quartz
2) New developments in measurement techniques
3) New findings concerning the trap structure